Molecular Pharmacology Fast Forward. Published on February 5, 2015 as DOI: 10.1124/mol.114.096495
This article has not been copyedited and formatted. The final version may differ from this version.

MOL #96495

Cannabinoid receptor interacting protein 1a ($CRIP_{1a}$) modulates CB_1 receptor signaling and regulation

Tricia H. Smith, Lawrence C. Blume, Alex Straiker, Jordan O. Cox, Bethany G. David, Julie Secor McVoy, Katherine W. Sayers, Justin L. Poklis, Rehab A. Abdullah, Michaela Egertová, Ching-Kang Chen, Ken Mackie, Maurice R. Elphick, Allyn C. Howlett and Dana E. Selley

Department of Pharmacology & Toxicology and Institute for Drug & Alcohol Studies, Virginia Commonwealth University School of Medicine, Richmond, VA 23298 (THS, JLP, RAA, JOC, BGD, JSM, DES).

Department of Physiology & Pharmacology, Wake Forest University Health Sciences, Winston-Salem, NC 27157 (LCB, ACH).

The Gill Center for Biomolecular Science and the Department of Psychological & Brain Sciences, Indiana University, Bloomington, Indiana 47405 (AS, KM).

Department of Anatomy & Neurobiology, Virginia Commonwealth University School of Medicine, Richmond, VA 23298 (KWS).

Department of Biochemistry & Molecular Biology, Virginia Commonwealth University School of Medicine, Richmond, VA 23298 (CKC).

School of Biological & Chemical Sciences, Queen Mary, University of London, London, United Kingdom (MRE, ME).

Molecular Pharmacology Fast Forward. Published on February 5, 2015 as DOI: 10.1124/mol.114.096495
This article has not been copyedited and formatted. The final version may differ from this version.

MOL #96495

Running title: $CRIP_{1a}$ modulates CB_1 receptor signaling and regulation

Corresponding author:

Dana E. Selley, PhD

Department of Pharmacology & Toxicology

Virginia Commonwealth University

Box 980524, McGuire Hall

1112 East Clay Street

Richmond, VA 23298-0524

Tel: (804) 827-0463

Fax: (804) 828-1532

E-mail: deselley@vcu.edu

Pages of text: 70

Number of tables: 5

Number of Figures: 10

Words in Abstract: 250

Words in Introduction: 747

Words in Discussion: 1500

Abbreviations: CB_1R, cannabinoid CB_1 receptor; $CRIP_{1a}$, cannabinoid receptor-interacting protein 1a; DSE, depolarization-induced suppression of excitation; EPSC, excitatory post-synaptic current; G-protein, guanine nucleotide-binding regulatory

Molecular Pharmacology Fast Forward. Published on February 5, 2015 as DOI: 10.1124/mol.114.096495
This article has not been copyedited and formatted. The final version may differ from this version.

protein; GPCR, G-protein-coupled receptor; GRK, G-protein-coupled receptor kinase; GASP1, G-protein-coupled receptor-associated sorting protein 1; GTPγS, guanylyl-5'-[*O*-thio]-triphosphate; HEK-293, human embryonic kidney 293; CPA, cyclopentyladenosine; CP55,940, (-)-*cis*-3-[2-hydroxy-4-(1,1-dimethylheptyl)phenyl]-*trans*-4-(3-hydroxypropyl)cyclohexanol; HU-210; 3-(1,1'- dimethylheptyl)-6αR,7,10,10αR-tetrahydro-1-hydroxy-6,6-dimethyl-6H-dibenzo[β,δ]pyran-9-methanol; MAEA, methanandamide, LEVO, levonantradol ([(6S,6αR,9R,10αR)-9-hydroxy-6-methyl-3-[(2R)-5-phenylpentan-2-yl]oxy- 5,6,6a,7,8,9,10,10α-octahydrophenanthridin-1-yl] acetate); THC, Δ^9-tetrahydrocannabinol, RIM, rimonabant, SR1141716A (5-(4-chlorophenyl)-1-(2,4-dichlorophenyl)-4- methyl-N-1-piperidinyl-1H-pyrazole-3-carboxamide); WIN, WIN55,212-2 ([(3R)-2,3-dihydro-5-methyl-3-(4-morpholinylmethyl)pyrrolo[1,2,3-de]-1,4-benzoxazin-6-yl]-1-naphthalenyl-methanone); 2-AG, 2-arachidonoylglycerol; 2-AGE, 2-arachidonoylglycerol ether.

Molecular Pharmacology Fast Forward. Published on February 5, 2015 as DOI: 10.1124/mol.114.096495
This article has not been copyedited and formatted. The final version may differ from this version.

Abstract

Cannabinoid CB_1 receptors (CB_1R) mediate the presynaptic effects of endocannabinoids in the central nervous system (CNS) and most behavioral effects of exogenous cannabinoids. Cannabinoid Receptor-Interacting Protein 1a ($CRIP_{1a}$) binds to the CB_1R C-terminus and can attenuate constitutive CB_1R-mediated inhibition of Ca^{2+} channel activity. We now demonstrate cellular co-localization of $CRIP_{1a}$ at neuronal elements in the CNS, and show that $CRIP_{1a}$ inhibits both constitutive and agonist-stimulated CB_1R-mediated G-protein activity. Stable over-expression of $CRIP_{1a}$ in HEK-293 cells stably expressing CB_1Rs (CB_1-HEK), or in N18TG2 cells endogenously expressing CB_1Rs, decreased CB_1R-mediated G-protein activation (measured by agonist-stimulated [^{35}S]GTPγS binding) in both cell lines, and attenuated inverse agonism by rimonabant in CB_1-HEK cells. Conversely, siRNA-mediated knockdown of $CRIP_{1a}$ in N18TG2 cells enhanced CB_1R-mediated G-protein activation. These effects were not due to differences in CB_1R expression or endocannabinoid tone because CB_1R levels did not differ between cell lines varying in $CRIP_{1a}$ expression, and endocannabinoid levels were undetectable (CB_1-HEK) or unchanged (N18TG2) by $CRIP_{1a}$ over-expression. In CB_1-HEK cells, 4-hour pretreatment with cannabinoid agonists downregulated CB_1Rs and desensitized agonist-stimulated [^{35}S]GTPγS binding. $CRIP_{1a}$ over-expression attenuated CB_1R downregulation without altering CB_1R desensitization. Finally, in cultured autaptic hippocampal neurons, $CRIP_{1a}$ over-expression attenuated both depolarization-induced suppression of excitation (DSE) and inhibition of excitatory synaptic activity induced by exogenous application of cannabinoid, but not adenosine A1 agonists. These results confirm that $CRIP_{1a}$ inhibits

Molecular Pharmacology Fast Forward. Published on February 5, 2015 as DOI: 10.1124/mol.114.096495
This article has not been copyedited and formatted. The final version may differ from this version.

constitutive CB_1R activity, and demonstrate that $CRIP_{1a}$ can also inhibit agonist-stimulated CB_1R signaling and downregulation of CB_1Rs. Thus, $CRIP_{1a}$ appears to act as a broad negative regulator of CB_1R function.

Molecular Pharmacology Fast Forward. Published on February 5, 2015 as DOI: 10.1124/mol.114.096495
This article has not been copyedited and formatted. The final version may differ from this version.

Introduction

Cannabinoid CB_1 receptors (CB_1Rs) mediate most central nervous system (CNS) effects of the phytocannabinoid Δ^9-tetrahydrocannabinol (THC) and the endocannabinoids (Howlett et al., 2002). CB_1Rs are G-protein-coupled receptors (GPCRs) that primarily activate $G_{i/o}$ proteins (Howlett et al., 2002) and are widely distributed throughout the CNS (Herkenham et al., 1991). CB_1Rs mediate synaptic plasticity via inhibition of neurotransmitter release (Kano et al., 2009) and regulate memory/cognition, motor activity, motivation, anxiety, appetite and energy balance (Howlett et al., 2002). Thus, in addition to mediating abuse-related effects of cannabinoids, CB_1Rs are attractive, albeit challenging, targets for drug discovery for the treatment of multiple CNS disorders (Pacher et al., 2006). However, prolonged CB_1R activation by direct agonists produces tolerance, dependence, perturbation of transcription factors and CB_1R adaptation (Lazenka et al., 2013; Smith et al., 2010). Therefore, there is a need to better understand the regulation of CB_1R signaling.

CB_1Rs also interact with regulatory proteins that modulate CB_1R function and mediate downstream signaling (Howlett et al., 2010; Smith et al., 2010). These proteins include ubiquitous GPCR regulators, such as GPCR kinase-3 (GRK3) and β-arrestin2, which mediate CB_1R desensitization and intracellular trafficking (Jin et al., 1999; Nguyen et al., 2012). Proteins that interact with a limited subset of receptor types include GPCR-associated sorting protein-1 (GASP1) and AP-3, which mediate CB_1R targeting to lysosomes (Martini et al., 2007; Rozenfeld and Devi, 2008). In addition, CB_1Rs interact with specific cannabinoid receptor-interacting proteins, $CRIP_{1a}$ and $CRIP_{1b}$, which are not known to interact with any other GPCR (Niehaus et al., 2007).

Molecular Pharmacology Fast Forward. Published on February 5, 2015 as DOI: 10.1124/mol.114.096495
This article has not been copyedited and formatted. The final version may differ from this version.

$CRIP_{1a/b}$ interact with the last nine amino acids of the CB_1R C-terminus, but not with the CB_2R (Niehaus et al., 2007). Both $CRIP_{1a/b}$ proteins are encoded by the *Cnrip1* gene, which contains four exons: 1, 2, 3a and 3b. Alternative spicing produces transcripts comprising exons 1, 2 and 3a ($CRIP_{1a}$) or 1, 2 and 3b ($CRIP_{1b}$). $CRIP_{1a}$ homologs are found throughout vertebrates, whereas $CRIP_{1b}$ appears to be limited to primates (Niehaus et al., 2007). The search for CB_1R C-terminal-interacting proteins was initiated because this region exhibited auto-inhibition of constitutive (agonist-independent) CB_1R activity, which was relieved by truncation of the distal C-terminus of the receptor (Nie and Lewis, 2001a; Nie and Lewis, 2001b). Indeed, electrophysiological recordings in superior cervical ganglion (SCG) neurons showed that expression of $CRIP_{1a}$, but not $CRIP_{1b}$, attenuated constitutive CB_1-mediated inhibition of calcium channels, revealed by elimination of the inverse agonist activity of rimonabant (SR141716A). However, co-expression of $CRIP_{1a}$ and CB_1Rs did not alter agonist-induced inhibition of calcium currents or CB_1R expression levels (Niehaus et al., 2007), suggesting that $CRIP_{1a}$ inhibits constitutive CB_1R activity.

$CRIP_{1a}$ is highly expressed in the brain (Niehaus et al., 2007), and some reports suggest that $CRIP_{1a}$ is regulated by seizure activity. Sclerotic hippocampi from epileptic patients exhibited reduced expression of mRNA for both $CRIP_{1a}$ and CB_1R (Ludanyi et al., 2008). In contrast, $CRIP_{1a}$ mRNA was elevated in rat hippocampus and cortex following kainic acid-induced seizures (Bojnik et al., 2012). These findings suggest $CRIP_{1a}$ involvement in modulating CB_1R function in the pathogenesis or neuroadaptive response to epilepsy. Furthermore, $CRIP_{1a}$ expression inhibited the neuroprotective

Molecular Pharmacology Fast Forward. Published on February 5, 2015 as DOI: 10.1124/mol.114.096495
This article has not been copyedited and formatted. The final version may differ from this version.

effects of a cannabinoid agonist, while conferring a neuroprotective effect to an antagonist, in a cultured neuronal model of glutamate excitotoxicity (Stauffer et al., 2011). To date, evidence supports functional interactions between $CRIP_{1a}$ and CB_1R in striatal GABAergic medium spiny neurons (Blume et al., 2013), glutamatergic hippocampal neurons (Ludanyi et al., 2008), and retinal presynaptic terminals (Hu et al., 2010). In addition, the *Cnrip1* gene is hypermethylated in certain colorectal cancers (Lind et al., 2011; Oster et al., 2011), further suggesting potentially important functions of $CRIP_{1a}$ in multiple physiological systems.

Despite the potential significance of $CRIP_{1a}$ as a novel player in the endocannabinoid system, relatively little is known about its function. The present study determined the effects of $CRIP_{1a}$ on constitutive and agonist-stimulated G-protein activation in CB_1R-expressing cells. Because $CRIP_{1a}$ binds to the CB_1R C-terminus, which interacts with regulatory proteins that mediate CB_1R desensitization and downregulation, the effects of $CRIP_{1a}$ on prolonged agonist-induced adaptation in CB_1R expression and signaling were also examined. To examine co-localization of $CRIP_{1a}$ with CB_1Rs in a defined neuronal population in the CNS, co-labeling studies were conducted in the cerebellum because both proteins are highly expressed in this region (Herkenham et al., 1991; Niehaus et al., 2007) and it plays a major role in cannabinoid dependence (Tzavara et al., 2000). Finally, to investigate the effects of $CRIP_{1a}$ on endocannabinoid function, its influence on depolarization-induced suppression of excitation (DSE) was examined in autaptic hippocampal neurons.

Molecular Pharmacology Fast Forward. Published on February 5, 2015 as DOI: 10.1124/mol.114.096495
This article has not been copyedited and formatted. The final version may differ from this version.

Materials and Methods

Chemicals. [^{35}S]GTPγS (1150-1300 Ci/mmol) was obtained from Perkin-Elmer Life and Analytical Sciences (Waltham, MA). [^{3}H]SR141716A (44.0 Ci/mmol) was purchased from GE Healthcare (Buckinghamshire, UK). WIN 55,212-2 (dissolved in ethanol), GDP, pertussis toxin, phenylmethanesulfonyl flouride (PMSF) and bovine serum albumin (BSA) were purchased from Sigma-Aldrich (St. Louis, MO). THC, CP55,940, levonanatradol, HU-210, noladin ether and SR141716A were provided as solutions in ethanol by the Drug Supply Program of the National Institute on Drug Abuse (NIDA, Rockville, MD). Methanandamide was purchased from Cayman Chemical (Ann Arbor, MI). Li-COR Odyssey infrared dye secondary antibodies were purchased from Li-COR Biosciences (Lincoln, NE). Alpha-tubulin antibody was purchased from Santa Cruz Biotechnology (Santa Cruz, CA). All other reagent grade chemicals were purchased from Sigma-Aldrich (St. Louis, MO).

Stable transfection and treatment of cultured cells.

Human embryonic kidney (HEK-293) cells stably expressing the human CB_1R subcloned into pcDNA3 vector (hCB_1-HEK) (Abood et al., 1997) were cultured in Dulbecco's Modified Eagle Medium, 1x high glucose (DMEM) containing 10% fetal bovine serum (FBS), 100 U/ml penicillin/100 µg/ml streptomycin (P/S), 0.25 mg/ml geneticin (G418) and 15mM HEPES. hCB_1-HEK cells stably co-transfected with $CRIP_{1a}$ subcloned into the pcDNA3.1*zeo* vector (hCB_1-HEK-$CRIP_{1a}$) (Niehaus et al., 2007) were cultured in the same media with the addition of 0.1 mg/ml zeocin.

Molecular Pharmacology Fast Forward. Published on February 5, 2015 as DOI: 10.1124/mol.114.096495
This article has not been copyedited and formatted. The final version may differ from this version.

Stable $CRIP_{1a}$ over-expression and knockdown N18TG2 cell clones were generated by transfecting (Lipofectamine 2000; Invitrogen) N18TG2 cells with either a pcDNA3.1-$CRIP_{1a}$ mouse cDNA plasmid for over-expression, or two different pRNATin-H1.2 siRNA-$CRIP_{1a}$ vectors for knockdown. The GenScript siRNA target finder program was used to select $CRIP_{1a}$ siRNA-target sequences. $CRIP_{1a}$ N18TG2 cell lines were generated by isolating and expanding G418-resistent single colonies in selection media containing 600 μg/ml G418 (Gibco Life Technologies). Cells were maintained in DMEM/HF12 media with 10% heat-inactivated bovine serum, GlutaMax, and P/S, with 0.25 mg/ml geneticin.

For ligand pretreatments, appropriate concentrations of drugs were added to treatment media (DMEM, 1% FBS, P/S) and sterile filtered, and drug treatment media was added to cells for the appropriate time period. To terminate drug treatments, cells were rinsed twice for 2 min with warm rinse media (DMEM, 1% FBS), and harvested for assays.

Membrane homogenate preparation. Cells were harvested in phosphate-buffered saline with 0.4% (w/v) EDTA or by gentle scraping and centrifuged at 1,000 x g for 10 min to remove media. Cells were homogenized in ice-cold 50 mM Tris-HCl, 3 mM $MgCl_2$ and 1 mM EGTA, pH 7.4, and centrifuged at 50,000 x g for 10 min. The resulting pellets were homogenized in 50 mM Tris-HCl, 3 mM $MgCl_2$, 0.2 mM EGTA, pH 7.4 (TME buffer) with 100 mM NaCl, and protein content was determined.

Cerebella were obtained from adult, male Sprague-Dawley rats (Harlan, Indianapolis, IN, U.S.A.). Rats were sacrificed by rapid decapitation, brains were removed and cerebella were dissected on ice. Cerebellum samples were homogenized in membrane

Molecular Pharmacology Fast Forward. Published on February 5, 2015 as DOI: 10.1124/mol.114.096495
This article has not been copyedited and formatted. The final version may differ from this version.

buffer and membranes were isolated by centrifugation as described above. Experiments were performed with the approval of the Institutional Animal Care and Use Committee at Virginia Commonwealth University in accordance with the National Institutes of Health guide for the care and use of Laboratory animals 7th edition.

$CRIP_{1a}$ generation, purification, and determination of stoichiometry. A $CRIP_{1a}$ cDNA insert was subcloned into the Bam HI and Xho I sites of the pGEX-4T-1 vector (GE Healthcare, Piscataway, NJ) to generate a glutathione-S-transferase (GST)-tagged $CRIP_{1a}$ (GST tag-thrombin cleavage site-$CRIP_{1a}$) construct. Plasmid DNA containing GST-tagged $CRIP_{1a}$ was transformed into *E. coli* BL21-DE3 competent cells. *E. coli* were grown to OD(600) = 0.6 from a single colony, and then GST-tagged $CRIP_{1a}$ expression was induced via addition of isopropyl thiogalactoside (IPTG, 1 mM) for 6 hours. *E. coli* were collected via centrifugation (1,000 g, 10 min, 4° C) and a bacterial lysate produced via sonication with lysozyme (25 µg/ml). $CRIP_{1a}$ induction and solubility tests were performed by polyacrylamide gel electrophoresis (PAGE) on harvested lysates using 10% polyacrylamide gels, which were stained with Coomassie blue to verify protein expression. Crude lysate was then separated into soluble and insoluble lysates. GST-tagged $CRIP_{1a}$ was isolated from bacterial lysate using a GSTrap FF column (Amersham Biosciences, Piscataway, NJ) as follows. The column was equilibrated with binding buffer (0.1 M phosphate buffered saline, PBS), bacterial lysate was added to allow GST-CRIP fusion, the column was washed (PBS), and the GST tag was cleaved via thrombin (500 units in 0.5 ml PBS). Following elution with PBS, $CRIP_{1a}$ was purified by the subsequent removal of thrombin using HiTrap Benzamidine column purification. Briefly, the column was equilibrated with binding

Molecular Pharmacology Fast Forward. Published on February 5, 2015 as DOI: 10.1124/mol.114.096495
This article has not been copyedited and formatted. The final version may differ from this version.

buffer (0.05 M Tris-HCl, 0.5 M NaCl, pH 7.4) and then the sample was added to the column followed by elution with binding buffer. $CRIP_{1a}$ eluates were collected and pooled, and $CRIP_{1a}$ pools and a BSA protein concentration curve were subjected to PAGE using 15% polyacrylamide gels, and visualized by Coomassie blue stain. Stained gel images were captured via Image J, and $CRIP_{1a}$ concentration was determined by subsequent linear regression analysis (Windows Excel). Purified $CRIP_{1a}$ concentration curves were then generated in tandem with hCB_1-HEK (± $CRIP_{1a}$) cell membrane preparations or rat cerebellar membranes to determine $CRIP_{1a}$ concentration via immunoblot analysis on 15% polyacrylamide gels. From these data, the stoichiometric relationship between $CRIP_{1a}$ concentration in cell membranes and CB_1R levels, determined by [^{3}H]SR141716A B_{max} values, was calculated.

Immunoblotting. Samples (70 μg) of cell membrane homogenates were added to sample buffer (1 M Tris-Cl, 20% Na dodecylsulfate (SDS), 1 M dithiothreitol (DTT), 60% sucrose, bromophenol blue) and boiled for 10 min. Samples were loaded into 15% SDS polyacrylamide gels, and electrophoresis was conducted at 120 V for 1.5 hours. Proteins were transferred by electrophoresis onto polyvinylidene difluoride (PVDF) membranes at 70 V for 70 min. Blots were blocked for 1 hour at room temperature (RT) with 5% (w/v) nonfat dry milk and then rinsed with TRIS buffered saline with 0.1% (v/v) Tween-20 (TBST). Primary antibody (rabbit anti-$CRIP_{1a}$ antiserum 077.4; 1:500) (Niehaus et al., 2007) was incubated overnight at 4° C, followed by TBST rinse. Secondary antibody (Li-COR goat anti-rabbit 800 CW IR dye, 1:5,000) was then incubated at room temperature for 1 hr, followed by TBST rinse. Blots were visualized with the Li-COR Odyssey system.

Molecular Pharmacology Fast Forward. Published on February 5, 2015 as DOI: 10.1124/mol.114.096495
This article has not been copyedited and formatted. The final version may differ from this version.

[^{3}H]SR141716A Binding. Saturation analysis of [^{3}H]SR141716A binding was performed by incubating 30 μg of membrane protein with 0.5-10 nM [^{3}H] SR141716A in TME with 0.5% (w/v) BSA, in a total volume of 0.5 ml ± 5 μM unlabeled SR141716A to determine non-specific binding. The assay was incubated for 90 min at 30° C and terminated by vacuum filtration through GF/B glass fiber filters that were pre-soaked in Tris buffer containing 0.5% (w/v) BSA. Bound radioactivity was determined using liquid scintillation spectrophotometry at 45% efficiency for [^{3}H].

[**^{3}H]CP55,940 Binding.** Saturation analysis of [^{3}H]CP55,940 binding was performed by incubating 100 μg of membrane protein with 0.2-8 nM [^{3}H]CP55,940 in TME (without NaCl) with 0.5% (w/v) BSA, in a total volume of 0.5 ml ± 5 μM unlabeled SR141716A to determine non-specific binding. The assay was incubated for 90 min at 30° C and terminated by vacuum filtration through GF/B glass fiber filters that were pre-soaked in Tris buffer containing 0.5% (w/v) BSA. Bound radioactivity was determined using liquid scintillation spectrophotometry at 45% efficiency for [^{3}H].

[^{35}S]GTPγS binding. Cell membrane preparations (10 μg protein) were incubated with various drugs, 100 mM NaCl, 0.1 % BSA, 10 μM (CB_1-HEK) or 20 μM (N18TG2) GDP and 0.1 nM [^{35}S]GTPγS in TME in 0.5 ml total volume, for 2 hr at 30° C. In some experimental conditions, 100 mM NaCl was omitted to increase constitutive receptor activity. Basal binding was assessed in the absence of agonist, and nonspecific binding was measured with 10 μM unlabeled GTPγS. The reaction was terminated by vacuum filtration through GF/B glass fiber filters. Bound radioactivity was determined by liquid

Molecular Pharmacology Fast Forward. Published on February 5, 2015 as DOI: 10.1124/mol.114.096495
This article has not been copyedited and formatted. The final version may differ from this version.

scintillation spectrophotometry at 95% efficiency for [^{35}S].

Liquid chromatography electrospray ionization tandem mass spectrometry (LC-MS-MS) analysis of endocannabinoids. Arachidonoylethanolamide (AEA) and 2-arachidonoylglycerol (2-AG), were measured using a method modified from Di Marzo et al. (Di Marzo et al., 2000). Briefly, 2 pmol of AEA-d8 and 2 nmol 2AG-d8 as deuterated internal standards were added to each sample. The endocannabinoids were extracted from the samples with 3 volumes chloroform/methanol (2/1, v,v containing 34.8 mg PMSF/ml) and a 0.73% (w,v) sodium chloride mixture. The organic phases from the three extractions were pooled and the organic solvents were evaporated to dryness with nitrogen. Dried samples were reconstituted in 100 µl of chloroform and mixed with 1 ml cold acetone to precipitate proteins. The mixtures were centrifuged and the upper layers were collected and evaporated to dryness with nitrogen. The extracts were reconstituted with 100 µl of methanol and placed in autosample vials for LC-MS-MS analysis. The AEA and 2-AG were separated and detected using a Shumadzu SCL HPLC system (Kyoto, Japan) with a Discovery® HS C18 Column 15cm x 2.1mm, 3µm (Supelco: Bellefonte, PA) kept at 40°C and an Applied Bio systems 3200 Q trap with a turbo V source for TurbolonSpray (Ontario, Canada) run in multiple reaction monitoring (MRM) mode. The mobile phase consisted of 10:90 water:methanol with 0.1% (w/v) ammonium acetate and 0.1% (v/v) formic acid. The flow rate was 0.3 ml/min and total run time was 10.00 min. The injection volume was 20 µl and the auto sampler temperature was set at 5°C. The mass spectrometer was run in Electrospray Ionization in positive mode. Ions were analyzed in multiple reaction monitoring mode and the following transitions were monitored: (348>62) and (348>91) for AEA; (356>62) for

Molecular Pharmacology Fast Forward. Published on February 5, 2015 as DOI: 10.1124/mol.114.096495
This article has not been copyedited and formatted. The final version may differ from this version.

AEA-d8; (379>287) and (379>269) for 2-AG; (387>96) for 2AG-d8. The standard curves for the samples were 0.039 – 1.25 pmol AEA and 0.063- 2.0 nmol 2-AG. The limit of detection and limit of quantification were set at 0.039 pmol for AEA and 0.063 nmol for 2-AG.

Hippocampal culture preparation. All procedures used in this study were approved by the Animal Care Committee of Indiana University and conform to the Guidelines of the National Institutes of Health on the Care and Use of Animals. Mouse (CD1 strain) hippocampal neurons isolated from the CA1-CA3 region were cultured on microislands as described previously (Bekkers and Stevens, 1991; Furshpan et al., 1976). Neurons were obtained from animals (age postnatal day 0-2) and plated onto a feeder layer of hippocampal astrocytes that had been laid down previously (Levison and McCarthy, 1991). Cultures were grown in high-glucose (20 mM) DMEM containing 10% horse serum, without mitotic inhibitors and used for recordings after 8 days in culture and for no more than three hours after removal from culture medium.

Electrophysiology. When a single neuron is grown on a small island of permissive substrate, it forms synapses—or “autapses”—onto itself. All experiments were performed on isolated autaptic neurons. Whole cell voltage-clamp recordings from autaptic neurons were carried out at room temperature using an Axopatch 200A amplifier (Axon Instruments, Burlingame, CA). The extracellular solution contained (in mM) 119 NaCl, 5 KCl, 2.5 $CaCl_2$, 1.5 $MgCl_2$, 30 glucose, and 20 HEPES. Continuous flow of solution through the bath chamber (~2 ml/min) ensured rapid drug application

Molecular Pharmacology Fast Forward. Published on February 5, 2015 as DOI: 10.1124/mol.114.096495
This article has not been copyedited and formatted. The final version may differ from this version.

and clearance. Drugs were typically prepared as stocks, and then diluted into extracellular solution at their final concentration and used on the same day.

Recording pipettes of 1.8-3 MΩ were filled with (in mM) 121.5 KGluconate, 17.5 KCl, 9 NaCl, 1 $MgCl_2$, 10 HEPES, 0.2 EGTA, 2 MgATP, and 0.5 LiGTP. Access resistance and holding current were monitored and only cells with both stable access resistance and holding current were included for data analysis. Conventional stimulus protocol: the membrane potential was held at –70 mV and excitatory postsynaptic currents (EPSCs) were evoked every 20 seconds by triggering an unclamped action current with a 1.0 ms depolarizing step. The resultant evoked waveform consisted of a brief stimulus artifact and a large downward spike representing inward sodium currents, followed by the slower EPSC. The size of the recorded EPSCs was calculated by integrating the evoked current to yield a charge value (in pC). Calculating the charge value in this manner yields an indirect measure of the amount of neurotransmitter released while minimizing the effects of cable distortion on currents generated far from the site of the recording electrode (the soma). Data were acquired at a sampling rate of 5 kHz.

DSE stimuli: After establishing a 10-20 second 0.5 Hz baseline, DSE was evoked by depolarizing to 0 mV for 50 msec, 100 msec, 300 msec, 500 msec, 1 sec, 3 sec and 10 sec, followed in each case by resumption of a 0.5 Hz stimulus protocol for 20-80+ seconds, allowing EPSCs to recover to baseline values. This approach allowed us to determine the sensitivity of the synapses to DSE induction.

Transfection of autaptic cultures. Neurons were transfected using a modified calcium phosphate-based method (Jiang et al., 2004). Briefly, plasmids for HA-tagged

Molecular Pharmacology Fast Forward. Published on February 5, 2015 as DOI: 10.1124/mol.114.096495
This article has not been copyedited and formatted. The final version may differ from this version.

$CRIP_{1a}$ and for the fluorescent marker mCherry (2 μg/well) were combined with 2M $CaCl_2$ and gradually added to HBS; the mixture was added to the serum-free neuronal media. Coverslips were incubated with this mixture in a separate well for 2.5 hours while extra media was placed in a 10% CO_2 incubator to induce equilibration. At the end of 2.5 hours, the reaction mixture was replaced with acidified serum-free media for 20 minutes. After this, cells were returned to their home wells.

Immunostaining of autaptic cultures. Autaptic neurons cultured on coverslips were transfected and prepared as described previously (Straiker et al., 2009). Briefly, paraformaldehyde-fixed neurons were incubated with an HA11 antibody overnight at 4°C and then washed six times with 0.1 M PBS. Cells were next incubated with fluorescein isothiocyanate (FITC)-conjugated donkey secondary antibody (anti-mouse, 1:100, Jackson ImmunoResearch Laboratories, Inc., West Grove, PA) for 1.5 hours at room temperature. Finally cover slips were washed, dried and mounted. Images were acquired with a Leica TCS SP5 confocal microscope (Leica Microsystems, Wetzlar, Germany) using Leica LAS AF software and a 63X oil objective. Images were processed using ImageJ (available at http://rsbweb.nih.gov/ij/) and/or Photoshop (Adobe Inc., San Jose, CA).

Immunostaining of rat brain sections. Tissue preparation and immunofluorescence labeling were conducted as described (Falenski et al., 2007) with minor modification. Adult male Sprague-Dawley rats (200–250 g) (Harlan, Indianapolis, IN, U.S.A.) were housed on a 12 h light/dark cycle in single cages and were provided with food and water ad libitum. Rats were injected with ketamine/xylazine (75 mg/kg, i.p.), flushed

Molecular Pharmacology Fast Forward. Published on February 5, 2015 as DOI: 10.1124/mol.114.096495
This article has not been copyedited and formatted. The final version may differ from this version.

transcardially with saline and perfused with 4% paraformaldehyde in 100 mM sodium phosphate buffer (pH 7.4). Brains were removed and post-fixed in the same fixative overnight, and then placed in sodium phosphate buffer + 30% sucrose for cryoprotection. Coronal sections of the cerebellum (20 µm) were cut on a cryostat maintained at -20°C and thaw-mounted onto gelatin-subbed slides. Sections were incubated for 30 min in phosphate-buffered saline (PBS) containing 0.1% Triton X100 and then for 1 hr in SuperBlock Blocking Buffer (SBB, Pierce, Rockford, IL) with 0.1% Triton X100. Sections were then incubated with rabbit anti-$CRIP_{1a}$-Ct (antiserum 077.4, 1:1000) and guinea pig anti-CB_1R-Ct (against CB_1R residues 401-473, 1:1000) in SBB for 72 hr, followed by incubation in appropriate secondary antibodies ($CRIP_{1a}$: Alexa-488, CB_1: Alexa-595; 1:200) for 1hr. Slides were washed, and coverslips were mounted using Vectashield (Vector, Burlingame, CA) and sealed with clear nail polish. Images were captured at 60x magnification on a Zeiss 700 laser scanning confocal microscope.

For immunolabeling of $CRIP_{1a}$ with visualization by immunohistochemistry, brains were removed and post-fixed in Bouin's fixative for 3 days at room temperature before embedding in paraffin wax. Coronal sections (10 µm) were cut and mounted on glass slides. Dewaxed sections were blocked with 5% normal goat serum / PBS with 0.2% Triton X-100 (PBST) and then incubated with 077.2 $CRIP_{1a}$ antiserum diluted 1:1000 in 5% normal goat serum in PBST. Bound antibodies were revealed by using the avidin-biotin complex, peroxidase method (Vector Laboratories). The specificity of immunostaining was established by testing antisera pre-absorbed with the

Molecular Pharmacology Fast Forward. Published on February 5, 2015 as DOI: 10.1124/mol.114.096495
This article has not been copyedited and formatted. The final version may differ from this version.

KPNETRSLMWVNKESFL peptide antigen (20 µM), which comprises the C-terminal region of the rat $CRIP_{1a}$ protein.

Immunostaining of mouse brain sections. GAD67-GFP mice were generated by Dr. Yuchio Yanagawa (Gunman University, Gunma, Japan (Tamamaki et al., 2003)). Brain sections were prepared from mice perfused with 4% paraformaldehyde. Brains were removed and immersed in 30% sucrose for 24-72 hours at 4°C. Tissue was then frozen in a freezing compound (OCT, Tissue-tek) and sectioned (15-30 µm) using a Leica CM1850 cryostat. Tissue sections were mounted onto Superfrost-plus slides, washed in PBS then treated with SEA BLOCK blocking buffer (Thermoscientific, Rockford, IL). Cells were treated overnight at 4°C with antibodies prepared in PBS and detergent (saponin, 0.1%). Secondary antibodies (Alexa 488, 495 or 647, anti-mouse, anti-rabbit or anti-guinea pig as appropriate, Invitrogen, Carlsbad, CA) were subsequently applied overnight at 4°C. Monoclonal SV2 and GAD65 antibodies were obtained from the Developmental Studies Hybridoma Bank (Iowa City, IA) and used at 1:500. The guinea pig CB_1 and $CRIP_{1a}$ antibodies were developed in-house and used at 1:300 and have been described previously (Berghuis et al., 2007; Hu et al., 2010). Images were acquired with a Leica TCS SP5 confocal microscope (Leica Microsystems, Wetzlar, Germany) using Leica LAS AF software and a 63X oil objective. Images were processed using ImageJ (available at http://rsbweb.nih.gov/ij/) and/or Photoshop (Adobe Inc., San Jose, CA). Images were modified only in terms of brightness and contrast.

Molecular Pharmacology Fast Forward. Published on February 5, 2015 as DOI: 10.1124/mol.114.096495
This article has not been copyedited and formatted. The final version may differ from this version.

Data analysis. Unless otherwise noted, all binding data are reported as mean values ± standard error of the mean (SEM) of at least three independent experiments performed in duplicate ([^{3}H]SR141716A and [^{3}H]CP55,940) or triplicate ([^{35}S]GTPγS). Data were analyzed using GraphPad/Prism v5.0 software. B_{max}, K_D, E_{max} and EC_{50}, values were determined by non-linear regression analysis. Non-linear regression was used to fit the data to the following equation: $B = (B_{max})(L)/(K_D + L)$ where B = the amount of [^{3}H]-ligand bound at each ligand concentration L. B_{max} is the maximal predicted amount of [^{3}H]-ligand bound, and K_D is the equilibrium dissociation constant for [^{3}H]-ligand binding. Saturation curve-fitting analysis for [^{3}H]SR141716A and [^{3}H]CP55,940 were weighted by 1/x (1/[^{3}H]-ligand concentration) because non-specific binding is relatively high for these cannabinoid ligands and increases linearly with [^{3}H]-ligand concentration. For studies of G-protein activation, E_{max} and log EC_{50} were similarly determined from log concentration-effect curves, where E is the % change in [^{35}S]GTPγS binding relative to basal binding at any given concentration of receptor ligand, E_{max} is the maximal % change from basal [^{35}S]GTPγS binding observed at maximally effective concentrations of ligand, and log EC_{50} is the $\log^{10}$ of the molar concentration of receptor ligand producing half-maximal modulation of [^{35}S]GTPγS binding. Statistical comparison was performed on log EC_{50} values, which were then transformed and reported as EC_{50} values. Basal [^{35}S]GTPγS binding is determined in the absence of receptor ligand. Net-stimulated [^{35}S]GTPγS binding is defined as agonist-stimulated minus basal binding. Percent stimulation is defined as (net stimulated binding/basal binding) x 100%.

Significance was determined using ANOVA and the post-hoc Newman-Keuls multiple comparison test for comparison of three or more conditions or by Student's t-test for

Molecular Pharmacology Fast Forward. Published on February 5, 2015 as DOI: 10.1124/mol.114.096495
This article has not been copyedited and formatted. The final version may differ from this version.

comparison of two conditions. In the few instances where unequal variance between groups was detected by F-test, Welch's correction for unequal variance was applied. Two-way ANOVA and the post-hoc Bonferroni test were used in experiments comparing two or more sets of independent variables. Results were considered statistically significant when the p value ≤ 0.05. All inferential statistics were performed using GraphPad/Prism v5.0d software.

Molecular Pharmacology Fast Forward. Published on February 5, 2015 as DOI: 10.1124/mol.114.096495
This article has not been copyedited and formatted. The final version may differ from this version.

Results

Stoichiometry of CB_1R and $CRIP_{1a}$ expression in stably transfected HEK-293 cells and rat cerebellum. Niehaus et al. (2007) previously showed that $CRIP_{1a}$ localizes to the cell membrane and interacts with the C-terminal tail of CB_1Rs without affecting CB_1R expression levels. To confirm that stable co-expression of $CRIP_{1a}$ did not affect CB_1R expression and to determine $CRIP_{1a}$:CB_1 expression ratios, CB_1R B_{max} values were obtained using [^{3}H]SR141716A saturation binding analysis (Supplemental Figure 1) in HEK-293 cells stably expressing CB_1Rs (CB_1-HEK) and the same CB_1-HEK cell line then stably transfected with $CRIP_{1a}$ (CB_1-HEK-$CRIP_{1a}$). Results showed no significant difference in CB_1R expression, as determined by [^{3}H]SR141716A B_{max} values, between CB_1-HEK cells with and without stable co-expression of $CRIP_{1a}$ (Table 1). Similarly, no difference in the K_D value of [^{3}H]SR141716A was observed between CB_1-HEK and CB_1-HEK-$CRIP_{1a}$ cell lines (Table 1). These results confirm that stable $CRIP_{1a}$ over-expression did not affect CB_1R expression or affinity for [^{3}H]SR141716A in CB_1-HEK cells.

The effect of $CRIP_{1a}$ on CB_1R function is likely to be determined in part by the molar ratio of $CRIP_{1a}$ to CB_1R. To determine the stoichiometric relationship of $CRIP_{1a}$ to CB_1R expression, quantitative immunoblot analysis of $CRIP_{1a}$ was performed. $CRIP_{1a}$ was purified using GST-pulldown methodology and $CRIP_{1a}$ concentration curves were included in immunoblots to determine unknown $CRIP_{1a}$ concentrations (Figure 1A). The C-terminally-directed $CRIP_{1a}$ antibody (Niehaus et al., 2007) produced relatively clean blots, with few or no extraneous labeling other than the 18 kDa band corresponding to $CRIP_{1a}$ (Supplemental Figure 2). Experimentally determined $CRIP_{1a}$ concentrations

Molecular Pharmacology Fast Forward. Published on February 5, 2015 as DOI: 10.1124/mol.114.096495
This article has not been copyedited and formatted. The final version may differ from this version.

were then compared to CB_1R B_{max} values to determine the molar stoichiometric relationship of $CRIP_{1a}$:CB_1Rs (Table 1). In CB_1-HEK cells, the molar ratio of $CRIP_{1a}$:CB_1 was less than 1 (0.34 ± 0.08), indicating that the CB_1R is in molar excess relative to $CRIP_{1a}$ natively expressed in CB_1-HEK cells. In CB_1-HEK-$CRIP_{1a}$ cells, $CRIP_{1a}$ was in molar excess to the CB_1R, with a $CRIP_{1a}$:CB_1R ratio of 5.44 ± 0.42, which was significantly different from CB_1-HEK cells. For comparison of expression ratios of $CRIP_{1a}$:CB_1R in a native tissue, [^{3}H]SR141716A saturation analysis and quantitative immunoblotting of $CRIP_{1a}$ were also conducted in rat cerebellar membranes (Table 1). Interestingly, rat cerebellum had a $CRIP_{1a}$:CB_1R molar ratio of 32.02 ± 4.39, indicating a greater molar excess of $CRIP_{1a}$ relative to the CB_1R than in the CB_1-HEK-$CRIP_{1a}$ cells. These results demonstrate that membranes from CB_1-HEK-$CRIP_{1a}$ cells express a significantly greater molar ratio of $CRIP_{1a}$:CB_1R than CB_1-HEK cells, but not greater than the ratio obtained in membranes from rat cerebellar homogenates.

The stoichiometry result in rat cerebellum is complicated by the question of whether $CRIP_{1a}$ is co-localized in the same cells with CB_1Rs in this tissue. Therefore, to determine whether CB_1Rs and $CRIP_{1a}$ are co-localized in rat cerebellum, brain sections were co-labeled with rabbit anti-$CRIP_{1a}$ (green) and guinea pig anti-CB_1R-Ct (red) antibodies (Figure 1C). Co-localization at this level of resolution of $CRIP_{1a}$ immunoreactivity (ir) with CB_1-ir is evident in the molecular layer. $CRIP_{1a}$-ir is also evident at lower levels in the granule cell layer, where CB_1-ir is seldom detected. In the Purkinje cell layer, intense CB_1R-ir can be seen in putative axon terminals, possibly from basket cells that are presynaptic to the unstained somata of Purkinje cells; little or no $CRIP_{1a}$-ir is evident in the axon terminals of basket cells. The widespread but

Molecular Pharmacology Fast Forward. Published on February 5, 2015 as DOI: 10.1124/mol.114.096495
This article has not been copyedited and formatted. The final version may differ from this version.

heterogeneous distribution of $CRIP_{1a}$ among rat cerebellar layers was confirmed by immunohistochemical staining visualized with peroxidase labeling, which was blocked by co-incubation with an antigen peptide corresponding to the C-terminal region of $CRIP_{1a}$ (Supplemental Figure 3). These results indicate that in the cerebellum, $CRIP_{1a}$ is putatively co-localized with CB_1Rs in axonal fibers arising from the glutamatergic granule cells that project throughout the molecular layer, while the granule cell layer also contains $CRIP_{1a}$ at lower levels.

To determine the localization of $CRIP_{1a}$ and its co-localization with CB_1Rs in specific cellular elements of the cerebellum, immunofluorescent labeling was performed in the GAD67-GFP mouse, which expresses green fluorescent protein in GABA-ergic neurons (Tamamaki et al., 2003), with co-staining of multiple subcellular markers. Using an antibody developed against $CRIP_{1a}$ (Hu et al. 2010), we examined the distribution of this protein in multiple cerebellar sub-regions. $CRIP_{1a}$ is widely distributed in the cerebellum, abundant in both the molecular and granular layers (Figure 2A-C), similar to what was detected in the rat using an independent antibody in Figure 1. In the molecular layer the staining substantially overlaps with synaptic vesicle 2 (SV2), a presynaptic marker (Figure 2D), consistent with a presynaptic localization. However, we also observed co-staining with GAD67-GFP positive processes, perhaps belonging to Purkinje cells (Figure 2E). $CRIP_{1a}$ was widely co-localized with CB_1R throughout the molecular layer (Figure 2F), but not in the pinceau region near Purkinje cells (e.g. arrowhead Figure 2F) where the most intense CB_1R expression is seen. Higher magnification images in the granule cell layer showed that $CRIP_{1a}$ is commonly co-localized with CB_1Rs (Figure 3A). Indeed most $CRIP_{1a}$ puncta overlapped with CB_1R-ir,

Molecular Pharmacology Fast Forward. Published on February 5, 2015 as DOI: 10.1124/mol.114.096495
This article has not been copyedited and formatted. The final version may differ from this version.

although there were some CB_1R-positive puncta that were not positive for $CRIP_{1a}$. The diffuse $CRIP_{1a}$ staining appeared to correspond to mossy terminal staining as shown by overlap with the brighter SV2 staining (Figure 3B). However the most punctate $CRIP_{1a}$ staining, seen when mossy terminal staining was allowed to saturate (Figure 3B2-4), also partially overlapped with SV2. $CRIP_{1a}$ staining in the granule cell layer did not co-localize with GAD65-ir (Figure 3C) or GAD67-GFP (data not shown), suggesting that expression is restricted to excitatory cells in the granule layer (Meyer et al., 2002). It is notable that $CRIP_{1a}$ is not detected in the pinceau region of basket cell inputs to the Purkinje neurons (Figure 3D), an area that is associated with strong CB_1R expression (e.g. Fig 2F). These results indicate widespread co-localization of $CRIP_{1a}$ with CB_1Rs in multiple cellular elements of the cerebellum, although $CRIP_{1a}$ and CB_1R expression did not completely overlap in all cerebellar sub-regions examined.

Effects of $CRIP_{1a}$ on CB_1R-mediated G-protein activation in stably transfected HEK-293 cells. To determine the effects of $CRIP_{1a}$ on CB_1R mediated G-protein activity, basal and ligand-modulated [^{35}S]GTPγS binding was conducted in CB_1-HEK (± $CRIP_{1a}$) cells (Figure 4). Concentration-effect curves for a variety of cannabinoid ligands were examined, including the classical phytocannabinoid THC, and its synthetic analogs HU210 and levonantradol, the aminoalkylindole WIN55,212-2, the bicyclic cannabinoid CP55,940, the eicosanoids noladin ether (2-arachidonoylglycerol ether; 2-AGE), a stable analog of 2-AG that is also a putative endocannabinoid, and methanandamide (MAEA), a stable analog of anandamide, and the diarylpyrazole inverse agonist rimonabant, also known as SR141716A. Non-linear regression fitting of

Molecular Pharmacology Fast Forward. Published on February 5, 2015 as DOI: 10.1124/mol.114.096495
This article has not been copyedited and formatted. The final version may differ from this version.

the concentration-effect curves revealed maximal stimulation (E_{max}) and EC_{50} values for each ligand (Table 2). Results in CB_1-HEK cells showed that noladin ether, WIN55,212-2 and HU210 appeared to act as full agonists (Figure 4; Table2). CP55,212-2 acted as a high efficacy partial agonist relative to 2-AGE, and MAEA and levonantradol were moderate efficacy partial agonists. THC acted as a low efficacy partial agonist and rimonabant acted as an inverse agonist (Figure 4; Table 2).

In agreement with our previous findings (Niehaus et al., 2007), stable $CRIP_{1a}$ expression reduced the apparent inverse agonism of rimonabant compared to CB_1-HEK cells without $CRIP_{1a}$ transfection (Figure 4), as indicated by a main effect of cell line in two-way ANOVA (cell line x ligand concentration) of the concentration-effect curves (Table 2). This reduction in inverse agonism was due to a lesser maximal inhibition of basal G-protein activation by rimonabant in CB_1-HEK-$CRIP_{1a}$ than in CB_1-HEK cells (Table 2). However, [^{35}S]GTPγS binding measured in the absence of cannabinoid ligand (basal) did not differ between cell types. Basal binding in CB_1-HEK cells was 89.8 ± 6.1 fmol/mg and in CB_1-HEK-$CRIP_{1a}$ cells was 86.4 ± 5.5 fmol/mg. Stable expression of $CRIP_{1a}$ also reduced stimulation of G-protein activation by the high efficacy agonists 2-AGE, WIN55,212-2, HU210 and CP55,940 (Figure 4; Table 2), as indicated by an effect of cell line in two-way ANOVA. This decrease in agonist-stimulated activity was due to a reduction in maximal stimulation (E_{max}) in CB_1-HEK-$CRIP_{1a}$ relative to CB_1-HEK cells, without any significant differences in EC_{50} values between the cell lines (Table 2).

Molecular Pharmacology Fast Forward. Published on February 5, 2015 as DOI: 10.1124/mol.114.096495
This article has not been copyedited and formatted. The final version may differ from this version.

Interestingly, concentration-effect curves for G-protein activation by the partial agonists MAEA, levonantradol and THC were unaffected by $CRIP_{1a}$ over-expression (Figure 4; Table 2). There was no significant effect of cell line in the presence of any of these partial agonists, and neither the E_{max} or EC_{50} values of these ligands differed between CB_1-HEK and CB_1-HEK-$CRIP_{1a}$ cells. Due to the differential effect of $CRIP_{1a}$ on G-protein activation by ligands of different intrinsic efficacies, the relative efficacy relationship among some ligands differed between cell types. In CB_1-HEK cells the order of descending relative efficacy, based on E_{max} values, was 2-AGE ≥ HU210 = WIN55,212-2 ≥ CP55,940 ≥ MAEA = levonantradol > THC >> rimonabant, whereas in CB_1-HEK-$CRIP_{1a}$ cells it was 2-AGE > HU210 > WIN55,212-2 = CP55,940 = MAEA = levonantradol > THC >> rimonabant.

The results described above indicate that stable $CRIP_{1a}$ expression in CB_1-HEK-$CRIP_{1a}$ cells did not inhibit basal [^{35}S]GTPγS binding or [^{3}H]SR141716A binding. However, $CRIP_{1a}$ inhibited the inverse agonist effects of rimonabant under conditions of high [Na^+], which reduces constitutive GPCR activity (Seifert and Wenzel-Seifert, 2002). We therefore determined whether $CRIP_{1a}$ inhibits constitutive receptor activity that is unrestricted by sodium. Results showed that 100 mM NaCl reduced basal [^{35}S]GTPγS binding in both CB_1-HEK and CB_1-HEK-$CRIP_{1a}$ cells by >50% relative to the absence of Na^+ (Figure 5A), as confirmed by 2-way ANOVA (effect of Na^+, $p < 0.0001$). To distinguish receptor-mediated from receptor-independent G-protein activity, cells were pretreated with or without pertussis toxin (PTX), which uncouples $G_{i/o}$-proteins from receptor-stimulated guanine nucleotide exchange (Sunyer et al., 1989). Na^+ also inhibited basal [^{35}S]GTPγS binding by 38% in both cell lines after treatment with PTX

Molecular Pharmacology Fast Forward. Published on February 5, 2015 as DOI: 10.1124/mol.114.096495
This article has not been copyedited and formatted. The final version may differ from this version.

(effect of sodium, $p < 0.0001$), but the effect was diminished relative to untreated cells (Figure 5B). Importantly, $CRIP_{1a}$ inhibited basal [^{35}S]GTPγS binding in untreated cells (effect of $CRIP_{1a}$, $p = 0.009$), but not in cells pretreated with PTX (no effect of $CRIP_{1a}$, $p = 0.496$). The inhibitory effect of $CRIP_{1a}$ on basal [^{35}S]GTPγS binding was significant only in untreated cells in the absence of Na^+, as confirmed by Bonferroni post-hoc analysis. These results indicate that $CRIP_{1a}$ inhibits spontaneous receptor-mediated G-protein activity, particularly in the absence of sodium, but does not affect receptor-independent [^{35}S]GTPγS binding.

To determine the effects of Na^+ on CB_1R ligand-modulated G-protein activity, net [^{35}S]GTPγS binding was determined in the presence of a maximally effective concentration of WIN55,212-2 or rimonabant with without 100 mM NaCl in CB_1-HEK and CB_1-HEK-$CRIP_{1a}$ cells. Na^+ enhanced net-stimulated [^{35}S]GTPγS binding by WIN55,212-2 (effect of Na^+, $p < 0.0001$), and there was a significant interaction between Na^+ and $CRIP_{1a}$ ($p = 0.0346$), as indicated by 2-way ANOVA (Figure 6A). In the absence of Na^+, WIN55,212-2 had no effect on [^{35}S]GTPγS binding. In contrast, WIN55,212-2 stimulated [^{35}S]GTPγS binding in the presence of 100 mM Na^+ ($p < 0.05$ by Bonferroni post-hoc test). The opposite effect of Na^+ was seen with rimonabant (Figure 6B). There was a significant effect of both Na^+ ($p = 0.0024$) and $CRIP_{1a}$ ($p = 0.0466$) on net rimonabant-inhibited [^{35}S]GTPγS binding by 2-way ANOVA. However, post-hoc analysis revealed that rimonabant only significantly inhibited [^{35}S]GTPγS binding in the absence of Na^+ ($p < 0.05$ by Bonferroni test). These results indicate that $CRIP_{1a}$ maximally attenuates agonist-stimulated [^{35}S]GTPγS binding in the presence of

Molecular Pharmacology Fast Forward. Published on February 5, 2015 as DOI: 10.1124/mol.114.096495
This article has not been copyedited and formatted. The final version may differ from this version.

high of [Na^+] and maximally attenuates inverse agonist-inhibited [^{35}S]GTPγS binding in the absence of Na^+, suggesting that $CRIP_{1a}$ attenuates both agonist-stimulated and constitutive CB_1R-mediated G-protein activation in a manner consistent with the effects of Na^+ on basal receptor activity seen in Figure 5.

A potential confounding factor in the interpretation of the effects of $CRIP_{1a}$ on basal CB_1R-mediated G-protein activity is the possible presence of endocannabinoids in the membrane preparation. To determine whether endocannabinoids are likely to have contributed to basal G-protein activity, mass spectrometric analysis of CB_1-HEK and CB_1-HEK-$CRIP_{1a}$ cells and isolated cell membranes was performed to quantify the two major endocannabinoids, 2-arachidonoyl glyercerol (2-AG) and anandamide (AEA). However, endocannabinoid levels were below the limit of detection for both 2-AG (>0.063 pmol) and AEA (>0.039 nmol) relative to deuterated standards, in extracts of both intact cells and isolated membranes, as determined in analysis of three independent samples. These results indicate that endocannabinoids are unlikely to have contributed to apparent basal CB_1R-mediated G-protein activity in either cell line.

Effect of $CRIP_{1a}$ on CB_1R desensitization and downregulation in stably transfected HEK-293 cells. To determine whether $CRIP_{1a}$ affected the regulation of CB_1R function by prolonged agonist occupancy, CB_1-HEK cells with and without stable $CRIP_{1a}$ co-transfection were pretreated with WIN55,212-2 (10 μM), THC (6 μM) or vehicle for 4 hours, followed by MAEA-stimulated [^{35}S]GTPγS binding to assess CB_1R function. MAEA was used to assess CB_1R activation after prolonged ligand pretreatment because acute stimulation of [^{35}S]GTPγS binding by this ligand was unaffected by

Molecular Pharmacology Fast Forward. Published on February 5, 2015 as DOI: 10.1124/mol.114.096495
This article has not been copyedited and formatted. The final version may differ from this version.

$CRIP_{1a}$ (Figure 2B; Table 2). Pretreatment of the cells with WIN55,212-2 or THC decreased CB_1R-mediated G-protein activation in membranes prepared from either cell line (Figure 7). Significantly lower MAEA E_{max} values were seen in WIN55,212-2-pretreated compared to vehicle-pretreated cells with or without $CRIP_{1a}$ co-transfection (Table 3A). In contrast, THC pretreatment did not affect MAEA E_{max} values in either cell line. However, pretreatment with either drug significantly increased MAEA EC_{50} values (Table 3A). Thus, pretreatment with either WIN55,212-2 or THC apparently desensitized MAEA-stimulated G-protein activity in both cell lines. However, there were no apparent differences in the level of desensitization produced by either ligand between CB_1-HEK cells with and without stable $CRIP_{1a}$ co-transfection. Indeed, two-way ANOVA of E_{max} values indicated a significant effect of drug pretreatment ($p < 0.0001$), but there was no effect of $CRIP_{1a}$ ($p = 0.306$). Similarly, two-way ANOVA of EC_{50} values revealed a significant effect of drug pretreatment ($p = 0.0036$), but there was no effect of $CRIP_{1a}$ ($p = 0.848$). Subsequent one-way ANOVA with post-hoc Newman-Keuls multiple comparison test revealed that neither E_{max} nor EC_{50} values of MAEA differed significantly between CB_1-HEK cells with and without stable $CRIP_{1a}$ co-transfection after WIN55,212-2 or THC pre-treatment. These results indicate that $CRIP_{1a}$ did not affect cannabinoid-induced CB_1R desensitization under these conditions.

Basal [^{35}S]GTPγS binding was not significantly affected by ligand pretreatment in either cell line (Supplemental Figure 4). Basal [^{35}S]GTPγS binding in vehicle-pretreated cells was 48.9 ± 9.2 and 43.9 ± 4.2 fmol/mg in cells without and with $CRIP_{1a}$ co-expression, respectively. There was no significant effect of pretreatment ($p = 0.584$) or $CRIP_{1a}$ expression ($p = 0.547$) with regard to basal [^{35}S]GTPγS binding, according to two-way

Molecular Pharmacology Fast Forward. Published on February 5, 2015 as DOI: 10.1124/mol.114.096495
This article has not been copyedited and formatted. The final version may differ from this version.

ANOVA. Similarly, one-way ANOVA revealed no significant effect of pretreatment in either cell line. These results indicate that the pretreatment ligand was sufficiently removed prior to assay, because residual agonist that might have remained in the membrane preparation from pretreated cells would be predicted to elevate the apparent "basal" level of [^{35}S]GTPγS binding,

In contrast, $CRIP_{1a}$ over-expression attenuated cannabinoid ligand-induced CB_1R downregulation, as determined using the identical pretreatment protocol that was used to examine effects on G-protein activation. Two-way ANOVA of [^{3}H]SR141716A B_{max} values revealed significant effects of ligand pretreatment ($p = 0.0001$) but no effect of $CRIP_{1a}$ expression ($p = 0.199$). However, there was a trend toward an interaction between these two factors ($p = 0.06$). With regard to [^{3}H]SR141716A K_D values, there was no effect of ligand pretreatment ($p = 0.812$) or $CRIP_{1a}$ expression ($p = 0.345$), nor was there an interaction ($p = 0.736$). In CB_1-HEK cells, pretreatment with either 10 µM WIN55,212-2 or 6 µM THC decreased the B_{max} value of [^{3}H]SR141716A binding by 53% and 74%, respectively (Table 3B), as determined by one-way ANOVA with post-hoc Dunnett's test. However, analysis of B_{max} values in CB_1-HEK-$CRIP_{1a}$ cells showed no significant effect of ligand pretreatment by one-way ANOVA ($p = 0.274$). Likewise, one-way ANOVA revealed no significant effects of pretreatment on K_D values in either CB_1-HEK ($p = 0.734$) or CB_1-HEK-$CRIP_{1a}$ ($p = 0.798$) cells. These results indicate that pretreatment with either WIN55,212-2 or THC significantly downregulated CB_1Rs in CB_1-HEK cells, but not in CB_1-HEK-$CRIP_{1a}$ cells. Moreover, the lack of effect of ligand pretreatment on [^{3}H]SR141716A K_D values in either cell line further indicates that the

Molecular Pharmacology Fast Forward. Published on February 5, 2015 as DOI: 10.1124/mol.114.096495
This article has not been copyedited and formatted. The final version may differ from this version.

effects of these pretreatments on CB_1R levels or activation of G-proteins were not due to insufficient removal of the pretreatment ligand prior to assay.

Effects of $CRIP_{1a}$ on CB_1R-mediated G-protein activation in stably transfected N18TG2 cells. Results in CB_1-HEK cells with and without stable co-transfection of $CRIP_{1a}$ indicated that $CRIP_{1a}$ negatively modulates constitutive and high efficacy agonist-stimulated G-protein activation by CB_1Rs. To determine whether similar effects could be demonstrated in a neural cell type, mouse neuroblastoma N18TG2 cells, which endogenously express CB_1Rs, were stably transfected with $CRIP_{1a}$. In addition, because N18TG2 cells endogenously express $CRIP_{1a}$ at moderate levels that are in excess of CB_1R levels (Supplemental Figure 5, Table 4), cell lines with stable transfection of siRNA against $CRIP_{1a}$ were also generated. Two cloned cell lines (OX1 and OX5) were isolated that stably over-expressed $CRIP_{1a}$ mRNA without any alteration in CB_1R mRNA (Supplemental Figure 5B). $CRIP_{1a}$ clones expressed 8:1 and 7:1 ($CRIP_{1a}$:CB_1R) cDNA ratios, respectively, as compared with a 1:7 ratio in untransfected N18TG2 cells (determined by qPCR using eno2 as a standard; Supplemental Figure 5A). Comparative immunoblots also indicated greater relative expression of $CRIP_{1a}$ protein in $CRIP_{1a}$-overexpressing clones compared to untransfected N18TG2 cells (Supplemental Figure 5C). Likewise, two clones (KD2C and KD2F) were isolated that exhibited siRNA-mediated knockdown of $CRIP_{1a}$ mRNA relative to untransfected N18TG2 cells, whereas cells transfected with empty siRNA vector did not exhibit $CRIP_{1a}$ knockdown (Supplemental Figure 5A). Immunoblot analysis showed that $CRIP_{1a}$ protein levels were reduced by 50-60% in siRNA knockdown clones relative to untransfected or vector control-transfected N18TG2 cells (Supplemental Figure 5C), but

Molecular Pharmacology Fast Forward. Published on February 5, 2015 as DOI: 10.1124/mol.114.096495
This article has not been copyedited and formatted. The final version may differ from this version.

CB_1R protein levels did not differ between any of these cell models (Supplemental Figure 5D).

To determine the precise level of membrane-delimited $CRIP_{1a}$ protein expression in $CRIP_{1a}$-OX N18TG2 clones for comparison with results in $CRIP_{1a}$ over-expressing CB_1-HEK cells, quantitative immunoblots using purified $CRIP_{1a}$ standards were then conducted in isolated membranes prepared from the two $CRIP_{1a}$-transfected clones and untransfected N18TG2 cells. Untransfected N18TG2 cells expressed 0.56 ± 0.06 pmol $CRIP_{1a}$ per mg of membrane protein, whereas clones OX1 and OX5 expressed 1.35 ± 0.16 pmol/mg and 1.28 ± 0.09 pmol/mg, respectively. The results of $CRIP_{1a}$ quantitative immunoblots were then compared with B_{max} values derived from cannabinoid radioligand binding assays in control and $CRIP_{1a}$ over-expressing N18TG2 cell lines to determine the stoichiometric ratio of $CRIP_{1a}$:CB_1 and the effect of $CRIP_{1a}$ over-expression on CB_1R B_{max} values. Due to low CB_1R expression levels in N18TG2 cells, [^{3}H]CP55,940 was used as the radioligand because it yielded greater specific:non-specific binding ratios than [^{3}H]SR141716A. Quantitative immunoblot and [^{3}H]CP55,940 binding analysis indicated that $CRIP_{1a}$ over-expressing N18TG2 clones have approximately a 2.3-2.5-fold increase in both $CRIP_{1a}$ protein expression and the $CRIP_{1a}$:CB_1 expression ratio, in comparison to untransfected N18TG2 cells (Table 4).

In line with findings from stable CB_1-HEK-$CRIP_{1a}$ cells, $CRIP_{1a}$ over-expression (clones OX1 and OX5) or knockdown (clone KD2C) did not alter the B_{max} values of [^{3}H]CP55,940 binding (Table 4), as determined by one-way ANOVA ($p = 0.899$). Likewise, [^{3}H]CP55,940 K_D values were not significantly affected by $CRIP_{1a}$ over-

Molecular Pharmacology Fast Forward. Published on February 5, 2015 as DOI: 10.1124/mol.114.096495
This article has not been copyedited and formatted. The final version may differ from this version.

expression or knockdown (p = 0.145 by one-way ANOVA; Table 4). These results demonstrate altered expression of $CRIP_{1a}$ protein without altering CB_1R density in both $CRIP_{1a}$ over-expressing and knockdown cells compared to control N18TG2 cells. It is noteworthy to mention that the relative increase in $CRIP_{1a}$:CB_1R ratios in $CRIP_{1a}$ over-expressing N18TG2 cells was less than that in the CB_1-HEK cell models, where $CRIP_{1a}$ over-expressing cells showed a 16-fold increase over control cells, as compared to ~2.5-fold increase in N18TG2-$CRIP_{1a}$ cells.

To determine whether $CRIP_{1a}$ over-expression in N18TG2 cells affected constitutive and agonist-stimulated G-protein activation by CB_1Rs, ligand concentration-effect curves for modulation of [^{35}S]GTPγS binding were examined using WIN55,212-2, MAEA and rimonabant in $CRIP_{1a}$ knockdown clone KD2C (N18-$CRIP_{1a}$-KD) and over-expressing clone OX1 (N18-$CRIP_{1a}$-OX) compared to untransfected N18TG2 cells. Basal [^{35}S]GTPγS binding did not differ significantly between N18TG2 (68.1 ± 6.0 fmol/mg), N18-$CRIP_{1a}$-KD (66.6 ± 16.6) and N18-$CRIP_{1a}$-OX cells (70.5 ± 5.9 fmol/mg). Results of ligand concentration-effect curves showed that $CRIP_{1a}$ over-expression decreased WIN55,212-2- and MAEA-stimulated [^{35}S]GTPγS binding relative to control N18TG2 cells (Figure 4). There was a significant effect of $CRIP_{1a}$ knockdown on [^{35}S]GTPγS binding stimulated by either WIN55,212-2 ($p < 0.0001$) or MAEA ($p < 0.0001$) in N18-$CRIP_{1a}$-KD (clone KD2C) relative to control N18TG2 cells, as revealed by two-way ANOVA of the concentration-effect curves. Likewise, two-way ANOVA revealed a significant effect of $CRIP_{1a}$ over-expression on [^{35}S]GTPγS binding stimulated by either WIN55,212-2 ($p < 0.0001$) or MAEA ($p < 0.0001$) in N18-$CRIP_{1a}$-OX (clone OX1) relative to control N18TG2 cells. In contrast, rimonabant did not reliably inhibit basal

Molecular Pharmacology Fast Forward. Published on February 5, 2015 as DOI: 10.1124/mol.114.096495
This article has not been copyedited and formatted. The final version may differ from this version.

[^{35}S]GTPγS binding in a concentration-dependent manner in any of the three N18TG2 cell lines examined under these experimental conditions (Figure 4), in contrast to results obtained in the CB_1-HEK cell models. Accordingly, there were no significant effects of either rimonabant concentration or $CRIP_{1a}$ expression levels in comparing the rimonabant concentration-effect curves among these three N18TG2 cell lines using two-way ANOVA. Similar results were obtained with all three ligands when comparing ligand-modulated [^{35}S]GTPγS binding in the other $CRIP_{1a}$ over-expressing (OX5) and knockdown (KD2F) clones to control N18TG2 cells (Supplemental Figure 6).

Non-linear regression analysis of the ligand concentration-effect curves showed that the E_{max} values of both WIN55,212-2 and MAEA were significantly higher in N18-$CRIP_{1a}$-KD relative to control N18TG2 cells (Table 5). Conversely, the WIN55,212-2 E_{max} value was lower in N18-$CRIP_{1a}$-OX cells compared to control N18TG2 cells. However, the MAEA E_{max} value did not differ significantly between N18-$CRIP_{1a}$-OX cells and control N18TG2 cells, but both WIN55212-2 and MAEA E_{max} values in N18-$CRIP_{1a}$-OX cells were significantly lesser than in N18-$CRIP_{1a}$-KD cells. In contrast, neither WIN55212-2 nor MAEA EC_{50} values were significantly altered by manipulation of $CRIP_{1a}$ expression levels in these N18TG2 cells lines. Moreover, because two-way ANOVA showed no significant effect of rimonabant concentration in these N18TG2 cell models, curve-fitting analysis was not performed with this ligand. These results indicate that $CRIP_{1a}$ knockdown enhances whereas $CRIP_{1a}$ over-expression attenuates agonist-stimulated G-protein activation mediated by CB_1Rs that are endogenously expressed in N18TG2 neuroblastoma cells.

Molecular Pharmacology Fast Forward. Published on February 5, 2015 as DOI: 10.1124/mol.114.096495
This article has not been copyedited and formatted. The final version may differ from this version.

Potential effects of $CRIP_{1a}$ on constitutive CB_1R-mediated G-protein activation could not be determined in the N18TG2 cells models because rimonabant did not significantly inhibit basal [^{35}S]GTPγS binding. It is possible, however, that endocannabinoids present in N18TG2 cells could have obscured the inhibitory effects of rimonabant on basal G-protein activity, perhaps by competing with rimonabant. To address this question, lipid fractions from N18TG2 and N18-$CRIP_{1a}$-OX cells, or membranes isolated from each cell line, were analyzed by mass spectrometry to determine the content of 2-AG and AEA. Results showed detectable levels of 2-AG in both intact cells and membrane preparations, although levels on a per-cell basis were approximately 7.5-fold greater in intact cells than isolated membranes (Supplemental Figure 7). Importantly, 2-AG levels did not differ between N18TG2 and N18-$CRIP_{1a}$-OX cells in fractions prepared from either intact cells or isolated membranes. To determine whether the higher 2-AG levels in intact cells compared to membranes were due to greater lipase activity in cells, the cells were incubated in the presence and absence of the diacylglycerol lipase inhibitor tetrahydrolipstatin (orlistat). Results showed that orlistat treatment significantly decreased 2-AG levels in intact cell preparations, but not in membranes (Figure S6). In intact cells, two-way ANOVA revealed a significant effect of orlistat ($p = 0.032$) but not $CRIP_{1a}$ over-expression ($p = 0.696$), and there was no significant interaction between the two factors ($p = 0.768$). In isolated membranes, there was only a non-significant trend toward an effect of orlistat ($p = 0.105$), and there was no effect of $CRIP_{1a}$ over-expression ($p = 0.574$) and no interaction between the two factors ($p = 0.860$). AEA levels were detectable in intact cells, but were approximately 0.02% of the levels detected for 2-AG, or approximately 0.01 pmol/10^7 cells (data not

Molecular Pharmacology Fast Forward. Published on February 5, 2015 as DOI: 10.1124/mol.114.096495
This article has not been copyedited and formatted. The final version may differ from this version.

shown). Two-way ANOVA revealed no effects of either $CRIP_{1a}$ over-expression ($p = 0.540$) or THL ($p = 0.452$), and there was no significant interaction (0.791). AEA levels in membrane preparations were below the limit of detection. These results suggest that differences in endocannabinoid levels were not responsible for the lack of inhibitory effects of rimonabant in membrane preparations from N18TG2 cells with and without over-expression of $CRIP_{1a}$.

Effects of $CRIP_{1a}$ on endocannabinoid signaling in hippocampal neuronal cultures. Results from both HEK and N18TG2 cell models indicate that $CRIP_{1a}$ can negatively modulate agonist-stimulated CB_1R activity at the level of G-protein activation. However, our previous results from isolated SCG neurons indicated that while $CRIP_{1a}$ over-expression attenuated constitutive CB_1R-mediated Ca^{2+} channel inhibition, it did not alter agonist-inhibited Ca^{2+} channel activity (Niehaus et al. 2007). Therefore, the effects of $CRIP_{1a}$ over-expression on synaptic function of CB_1Rs were examined in a more CNS-relevant model. Autaptic hippocampal neurons express all the components of a functional cannabinoid signaling system, including presynaptic CB_1Rs, depolarization-dependent production of endocannabinoids, likely 2-AG (Straiker and Mackie, 2005), and monacylglycerol lipase (MAGL), which hydrolyzes 2-AG and thereby controls the duration of cannabinoid signaling (Straiker et al., 2009). To assess whether $CRIP_{1a}$ can functionally interact with this endogenous cannabinoid signaling system, $CRIP_{1a}$ was over-expressed in autaptic neurons. The distribution of $CRIP_{1a}$ protein was determined in transfected neurons using an HA11 antibody against the HA tag on the $CRIP_{1a}$ protein, and results showed that $CRIP_{1a}$ was widely expressed throughout the transfected neuron (Figure 9A). This widespread cellular localization was similar to that

Molecular Pharmacology Fast Forward. Published on February 5, 2015 as DOI: 10.1124/mol.114.096495
This article has not been copyedited and formatted. The final version may differ from this version.

of endogenous $CRIP_{1a}$ (Figure 9B, D compared to Figures 1, 2, and 3). Although endogenously expressed CB_1R appeared to be primarily limited to neuronal processes and putative autaptic terminals (Figure 9B, E), endogenous $CRIP_{1a}$ was widely co-localized in these cellular elements with CB_1Rs (Figure 9B, F). These results suggest that $CRIP_{1a}$ is spatially positioned in a manner such that it could modulate CB_1R function.

To determine whether $CRIP_{1a}$ over-expression altered the sensitivity of DSE induction in these autaptic hippocampal neurons, depolarization duration-response curves were obtained. Neurons were depolarized for progressively longer durations (50 msec, 100 msec, 300 msec, 500 msec, 1 sec, 3 sec and 10 sec) and the resulting CB_1R-dependent inhibition was measured. Results showed that the depolarization duration-response curve in $CRIP_{1a}$ over-expressing neurons differed substantially from that of control conditions, with a diminished inhibition at 1-, 3- and 10-second depolarizations (Fig 10A, B, $p < 0.05$ by Bonferroni post-hoc test after two-way ANOVA).

2-AG is a strong candidate to serve as the endocannabinoid mediating DSE (and DSI) at autaptic hippocampal synapses (Jain et al., 2013; Straiker and Mackie, 2005; Straiker and Mackie, 2009). Therefore, the response in $CRIP_{1a}$-transfected neurons to 2-AG was examined to determine whether sensitivity to exogenously added 2-AG was diminished similarly to DSE. Figure 10C shows that inhibition of EPSCs by 2-AG (5 µM) was substantially attenuated in $CRIP_{1a}$ over-expressing neurons relative to controls (relative EPSC charge with 2-AG (5 µM) treatment in WT neurons: 0.34 ± 0.03, n=4; in $CRIP_{1a}$-transfected neurons: 0.82 ± 0.06, n=7; $p < 0.05$ by unpaired t-test). We have

Molecular Pharmacology Fast Forward. Published on February 5, 2015 as DOI: 10.1124/mol.114.096495
This article has not been copyedited and formatted. The final version may differ from this version.

previously reported that anandamide activates CB_1Rs to inhibit neurotransmitter release in excitatory and inhibitory autaptic neurons (Straiker et al., 2009; Straiker and Mackie, 2005). Thus, the hydrolysis-resistant analog, MAEA, was tested under control and $CRIP_{1a}$-transfected conditions. As with 2-AG, $CRIP_{1a}$ over-expression similarly diminished MAEA signaling (Figure 10C, relative EPSC charge with MAEA (5 µM) treatment in WT neurons: 0.57 ± 0.03, n=4; in $CRIP_{1a}$-transfected neurons: 0.91 ± 0.11, n=5; $p < 0.05$ by unpaired t-test). To determine whether $CRIP_{1a}$ over expression would suppress constitutive inhibition of EPSCs by CB_1Rs, the effects of rimonabant (100 nM) were examined. However, no effect of this inverse agonist was detected regardless of whether or not $CRIP_{1a}$ was over-expressed (data not shown), as previously reported for non-transfected hippocampal autaptic cultures (Straiker et al., 2012).

To ascertain whether $CRIP_{1a}$ transfection interfered more generally with $G_{i/o}$-mediated modulation of neurotransmission, inhibition by the adenosine A_1 receptor agonist cyclopentyladenosine (CPA) was examined, because it was previously found to robustly inhibit EPSCs in autaptic hippocampal neurons (Straiker et al., 2002). Figure 10C shows that $CRIP_{1a}$ over-expression did not interfere with CPA responses (relative EPSC charge after treatment with CPA (100nM) in control neurons: 0.27 ± 0.03, n=10; in $CRIP_{1a}$-transfected neurons: 0.29 ± 0.06, n=4). Together, these results indicate that $CRIP_{1a}$ attenuates the inhibition of excitatory synaptic transmission by endocannabinoids, and that this action of $CRIP_{1a}$ is selective for modulation of synaptic transmission by CB_1Rs.

Molecular Pharmacology Fast Forward. Published on February 5, 2015 as DOI: 10.1124/mol.114.096495
This article has not been copyedited and formatted. The final version may differ from this version.

Discussion

This study extends the findings that $CRIP_{1a}$ attenuates constitutive inhibition of Ca^{2+} channels by CB_1Rs in co-transfected SCG neurons (Niehaus et al., 2007). Here we showed that $CRIP_{1a}$ attenuated rimonabant-mediated inhibition of basal [^{35}S]GTPγS binding in $CRIP_{1a}$ over-expressing CB_1-HEK cells, suggesting that $CRIP_{1a}$ over-expression disrupts constitutive CB_1R-mediated G-protein activation. $CRIP_{1a}$ over-expression also inhibited basal [^{35}S]GTPγS binding in CB_1-HEK cells in the absence of Na^+, but not in the presence of Na^+ or in PTX-pretreated cells, further indicating that $CRIP_{1a}$ inhibits CB_1R constitutive activity. There was an opposing effect of Na^+ on agonist- versus inverse agonist-modulated G-protein activity such that inverse agonism was maximized in the absence of Na^+, a condition under which PTX-sensitive basal G-protein activity was highest. Conversely, agonist-stimulated G-protein activation was maximized by 100 mM Na^+, a condition under which PTX-sensitive basal G-protein activation was minimal. $CRIP_{1a}$ over-expression suppressed the inverse agonist activity of rimonabant in the absence of Na^+, whereas $CRIP_{1a}$ only suppressed agonist-stimulated G-protein activation with Na^+ present. The absence of endocannabinoids in CB_1-HEK membranes suggests that $CRIP_{1a}$ effects did not result from dampening endocannabinoid tone. Altogether, these results indicate that $CRIP_{1a}$ over-expression inhibits constitutive and agonist-stimulated G-protein activity in CB_1-HEK cells in a manner consistent with the behavior of receptor-G-protein complexes with under the allosteric modulatory influence of Na^+ (Seifert and Wenzel-Seifert, 2002).

Molecular Pharmacology Fast Forward. Published on February 5, 2015 as DOI: 10.1124/mol.114.096495
This article has not been copyedited and formatted. The final version may differ from this version.

If $CRIP_{1a}$ regulates constitutive activity of CB_1Rs *in vivo*, then it can be hypothesized to modulate both cellular trafficking of CB_1Rs and pharmacological responses to inverse agonists. Constitutive activity may be required for CB_1R internalization and targeting to pre-synaptic terminals (Leterrier et al. 2004, 2006), although this has been disputed (McDonald et al., 2007). However, confirmation of constitutive CB_1R activity in the CNS has been elusive. For example, rimonabant concentrations necessary to depress basal G-protein activity in brain are greater than those required to antagonize CB_1 agonist-stimulated activity (Sim-Selley et al., 2001), and high rimonabant concentrations decrease basal G-protein activity in CB_1R knockout mice (Breivogel et al., 2001). $CRIP_{1a}$ over-expression inhibits constitutive CB_1R activity in CB_1-HEK cells, so it is possible that $CRIP_{1a}$ contributes to the low level of constitutive activity in the brain. This would be consistent with our finding that inverse agonism by rimonabant was not detected in N18TG2 cells, where endogenous $CRIP_{1a}$ might suppress constitutive CB_1R activity. Although siRNA-mediated knockdown of $CRIP_{1a}$ did not significantly enhance inverse agonism by rimonabant in N18TG2 cells, this finding could be due to the low CB_1R expression level and the fact that rimonabant was only examined in the presence of 100 mM Na^+ in these cells. Inhibition of basal [^{35}S]GTPγS binding by rimonabant in N18TG2 cells is minimal with Na^+ present, but detectable after replacement of Na^+ with K^+ (Meschler et al., 2000). Thus, these neural cell models will be useful to investigate CB_1R inverse agonism and the role of endogenous $CRIP_{1a}$ using varying cation concentrations in future studies.

Molecular Pharmacology Fast Forward. Published on February 5, 2015 as DOI: 10.1124/mol.114.096495
This article has not been copyedited and formatted. The final version may differ from this version.

The present study also confirmed that differences in $CRIP_{1a}$ expression do not influence total CB_1R expression levels or ligand binding affinity (Niehaus et al., 2007) in both HEK-293 and N18TG2 cell models, despite using different radioligands in each cell line. The finding of similar results with both antagonist/inverse agonist ([^{3}H]SR141716A) and agonist ([^{3}H]CP55,940) radioligands suggests that $CRIP_{1a}$ might influence CB_1R signaling efficacy without affecting the formation of high-affinity receptor-G-protein complexes, which will be addressed in future studies.

The effect of $CRIP_{1a}$ on CB_1R-mediated G-protein activation was dependent on the stoichiometric relationship between $CRIP_{1a}$ and CB_1Rs. In CB_1-HEK cells, stable $CRIP_{1a}$ transfection increased the $CRIP_{1a}$:CB_1R expression ratio from <0.5 to approximately 7. In N18TG2 cells, which endogenously express both proteins, $CRIP_{1a}$ transfection increased the ratio of $CRIP_{1a}$:CB_1R from approximately 2 to 5. Importantly, $CRIP_{1a}$ expression levels in both over-expressed cell lines were lower than in rat cerebellum, suggesting that these cells do not express supraphysiological $CRIP_{1a}$ levels relative to native tissues. Whether the ratio of over-expressed $CRIP_{1a}$:CB_1R is supraphysiological is difficult to ascertain because $CRIP_{1a}$ was more widely distributed throughout rat and mouse cerebellum than CB_1Rs, although co-localization was observed throughout the molecular and granule cell layers.

A major finding of the present study is that $CRIP_{1a}$ over-expression attenuated cannabinoid agonist-stimulated G-protein activation in both CB_1-HEK and N18TG2 cells. This result was not likely due to unnaturally over-expressed levels of $CRIP_{1a}$

Molecular Pharmacology Fast Forward. Published on February 5, 2015 as DOI: 10.1124/mol.114.096495
This article has not been copyedited and formatted. The final version may differ from this version.

because the opposite effect – enhancement of agonist-stimulated G-protein activity – was observed with siRNA-mediated knockdown of $CRIP_{1a}$ in N18TG2 cells. $CRIP_{1a}$ knockdown was not examined in CB_1-HEK cells because CB_1Rs were more highly expressed than $CRIP_{1a}$ in this model. Although the inhibitory effect of $CRIP_{1a}$ over-expression on maximal agonist-stimulated G-protein activation was moderate (~20-40%) in either cell line, a robust effect of $CRIP_{1a}$ was observed when comparing N18TG2 cells with $CRIP_{1a}$ knocked down versus over-expressed, whereby up to a 2.5-fold difference in agonist E_{max} values was observed. These results indicate that $CRIP_{1a}$ exerts a dramatic effect on CB_1R-mediated G-protein signaling under appropriate stoichiometric conditions. Moreover, $CRIP_{1a}$ over-expression in autaptic hippocampal neurons attenuated both DSE and inhibition of excitatory synaptic currents by 2-AG and MAEA, demonstrating that $CRIP_{1a}$ can regulate one of the most critical functions of CB_1Rs in neurons. In addition, $CRIP_{1a}$ over-expression did not alter synaptic inhibition by an adenosine A_1 agonist, suggesting that $CRIP_{1a}$ selectively modulates CB_1R activity without altering activity of other GPCRs. Altogether, these results suggest that $CRIP_{1a}$ could be an important modulator of endocannabinoid signaling in the CNS.

The effects of $CRIP_{1a}$ on CB_1R-mediated G-protein activation were also found to be ligand-dependent in CB_1-HEK cells. $CRIP_{1a}$ over-expression inhibited G-protein activation by agonists of high intrinsic efficacy, including 2-AGE, WIN55,212-2, HU-210 and CP55,940, but not ligands of lower intrinsic efficacy, including MAEA, levonantradol and THC. This effect was probably not related solely to chemotype because HU-210 and THC are classical cannabinoids whereas 2-AGE and MAEA are eicosanoids, yet

Molecular Pharmacology Fast Forward. Published on February 5, 2015 as DOI: 10.1124/mol.114.096495
This article has not been copyedited and formatted. The final version may differ from this version.

$CRIP_{1a}$ only affected the ligand with highest intrinsic efficacy in each class. It is possible that association of $CRIP_{1a}$ with CB_1Rs is modulated by the presence of bound ligand in an efficacy-dependent manner. This ligand-selective action of $CRIP_{1a}$ was also dependent on cell type because $CRIP_{1a}$ attenuated signaling induced by MAEA in both N18TG2 cells and hippocampal neurons, but not CB_1-HEK cells. Thus, the effects of $CRIP_{1a}$ on CB_1R-G-protein interactions could be dependent on G-protein subtype, which varies among cell types (Atwood et al., 2011). Previous work demonstrated differential association of distinct $G\alpha_{i/o}$ subtypes with CB_1Rs occupied by different ligands (Mukhopadhyay and Howlett 2005) and differential abilities of different ligands to activate purified G_i versus G_o (Glass and Northup, 1999). In addition, different $G\alpha_{i/o}$ subtypes interact selectively with either the C-terminus or third intracellular loop of the CB_1R (Anavi-Goffer et al., 2007; Mukhopadhyay and Howlett, 2001), so $CRIP_{1a}$ association with the CB_1R C-terminus (Niehaus et al., 2007) might differentially interfere with G-protein association with these distinct intracellular domains of the CB_1R. Because the C-terminus serves as a docking site for multiple protein-protein interactions (Howlett et al., 2010; Smith et al., 2010), the effects of $CRIP_{1a}$ on CB_1R-G-protein interactions might depend on both ligand occupancy of the receptor and the presence of additional interacting proteins.

The CB_1R C-terminus interacts with proteins that mediate desensitization and downregulation. For example, likely GRK phosphorylation sites have been identified (Daigle et al., 2008; Hsieh et al., 1999; Jin et al., 1999) and isolated fragments of the CB_1R C-terminus can bind to β-arrestins (Bakshi et al., 2007; Singh et al., 2011) and

Molecular Pharmacology Fast Forward. Published on February 5, 2015 as DOI: 10.1124/mol.114.096495
This article has not been copyedited and formatted. The final version may differ from this version.

GASP1 (Martini et al., 2007). Prolonged agonist exposure downregulates CB_1Rs expressed in HEK-293 (Shapira et al., 2003) but not N18TG2 cells (McIntosh et al., 1998). Therefore, we examined the effects of prolonged agonist exposure in CB_1-HEK cells, with and without $CRIP_{1a}$ over-expression, on CB_1R levels and agonist-induced activation of G-proteins. Interestingly, our results showed that $CRIP_{1a}$ over-expression interfered with CB_1R downregulation (degradation) but not desensitization (uncoupling from G-protein activation). These findings suggest that $CRIP_{1a}$ might interfere with GASP1 association with CB_1Rs (Martini et al., 2010; Martini et al., 2007) or with C-terminal CB_1R phosphorylation at sites that mediate internalization (Daigle et al., 2008; Jin et al., 1999), but not at sites that mediate desensitization (Jin et al., 1999; Morgan et al., 2014). Regional differences in CB_1R downregulation after repeated cannabinoid administration have been observed in the CNS of rodents (Sim-Selley, 2003; Sim-Selley et al., 2006) and humans (Hirvonen et al., 2012; Villares, 2007). Thus, differential co-localization of CB_1Rs with $CRIP_{1a}$ could contribute to regional differences in CB_1R downregulation, and might thereby influence the development of differential tolerance to distinct pharmacological effects of cannabinoids.

The present study provides evidence that $CRIP_{1a}$ attenuates constitutive and agonist-induced G-protein activation by CB_1Rs in two distinct cell lines, HEK-293 and N18TG2. Additionally, $CRIP_{1a}$ inhibits DSE in autaptic hippocampal neurons, suggesting that $CRIP_{1a}$ modulates the physiological actions of endocannabinoids in the CNS. These results indicate that $CRIP_{1a}$ is a negative regulator of acute CB_1R-mediated G-protein signaling. $CRIP_{1a}$ also attenuated agonist-induced CB_1R downregulation, suggesting

Molecular Pharmacology Fast Forward. Published on February 5, 2015 as DOI: 10.1124/mol.114.096495
This article has not been copyedited and formatted. The final version may differ from this version.

that it might oppose the development of cannabinoid tolerance. Thus, $CRIP_{1a}$ could play an important regulatory role in the endocannabinoid system by differentially modulating acute versus chronic activation of CB_1Rs.

Molecular Pharmacology Fast Forward. Published on February 5, 2015 as DOI: 10.1124/mol.114.096495
This article has not been copyedited and formatted. The final version may differ from this version.

Acknowledgements

The authors thank Hengjun He and Elizabeth Krahn for technical assistance, and Dr. Laura J. Sim-Selley and Erica C. Lyons for critical review of the manuscript.

Authorship Contributions:

Participated in research design: Smith, Blume, Straiker, Sayers, Poklis, Abdullah, Chen, Mackie, Howlett, Selley.

Conducted experiments: Smith, Blume, Straiker, David, McVoy, Sayers, Poklis, Abdullah, Cox, Egertová.

Contributed new reagents or analytic tools: Blume, Chen, Elphick, Mackie, Howlett

Performed data analysis: Smith, Blume, Straiker, David, McVoy, Poklis, Cox, Selley.

Wrote or contributed to the writing of the manuscript: Smith, Blume, Straiker, Sayers, Abdullah, Elphick, Mackie, Howlett, Selley

Molecular Pharmacology Fast Forward. Published on February 5, 2015 as DOI: 10.1124/mol.114.096495
This article has not been copyedited and formatted. The final version may differ from this version.

References

Abood ME, Ditto KE, Noel MA, Showalter VM and Tao Q (1997) Isolation and expression of a mouse CB1 cannabinoid receptor gene. Comparison of binding properties with those of native CB1 receptors in mouse brain and N18TG2 neuroblastoma cells. *Biochem Pharmacol* **53**(2): 207-214.

Anavi-Goffer S, Fleischer D, Hurst DP, Lynch DL, Barnett-Norris J, Shi S, Lewis DL, Mukhopadhyay S, Howlett AC, Reggio PH and Abood ME (2007) Helix 8 Leu in the CB1 cannabinoid receptor contributes to selective signal transduction mechanisms. *The Journal of biological chemistry* **282**(34): 25100-25113.

Atwood BK, Lopez J, Wager-Miller J, Mackie K and Straiker A (2011) Expression of G protein-coupled receptors and related proteins in HEK293, AtT20, BV2, and N18 cell lines as revealed by microarray analysis. *BMC genomics* **12**: 14.

Bakshi K, Mercier RW and Pavlopoulos S (2007) Interaction of a fragment of the cannabinoid CB1 receptor C-terminus with arrestin-2. *FEBS Lett* **581**(25): 5009-5016.

Bekkers JM and Stevens CF (1991) Excitatory and inhibitory autaptic currents in isolated hippocampal neurons maintained in cell culture. *Proc Natl Acad Sci U S A* **88**(17): 7834-7838.

Berghuis P, Rajnicek AM, Morozov YM, Ross RA, Mulder J, Urban GM, Monory K, Marsicano G, Matteoli M, Canty A, Irving AJ, Katona I, Yanagawa Y, Rakic P, Lutz B, Mackie K and Harkany T (2007) Hardwiring the brain: endocannabinoids shape neuronal connectivity. *Science* **316**(5828): 1212-1216.

Molecular Pharmacology Fast Forward. Published on February 5, 2015 as DOI: 10.1124/mol.114.096495
This article has not been copyedited and formatted. The final version may differ from this version.

Blume LC, Bass CE, Childers SR, Dalton GD, Roberts DC, Richardson JM, Xiao R, Selley DE and Howlett AC (2013) Striatal CB1 and D2 receptors regulate expression of each other, CRIP1A and delta opioid systems. *Journal of neurochemistry* **124**(6): 808-820.

Bojnik E, Turunc E, Armagan G, Kanit L, Benyhe S, Yalcin A and Borsodi A (2012) Changes in the cannabinoid (CB1) receptor expression level and G-protein activation in kainic acid induced seizures. *Epilepsy research* **99**(1-2): 64-68.

Breivogel CS, Griffin G, Di Marzo V and Martin BR (2001) Evidence for a new G protein-coupled cannabinoid receptor in mouse brain. *Molecular pharmacology* **60**(1): 155-163.

Daigle TL, Kwok ML and Mackie K (2008) Regulation of CB1 cannabinoid receptor internalization by a promiscuous phosphorylation-dependent mechanism. *Journal of neurochemistry* **106**(1): 70-82.

Di Marzo V, Breivogel CS, Tao Q, Bridgen DT, Razdan RK, Zimmer AM, Zimmer A and Martin BR (2000) Levels, metabolism, and pharmacological activity of anandamide in CB(1) cannabinoid receptor knockout mice: evidence for non-CB(1), non-CB(2) receptor-mediated actions of anandamide in mouse brain. *Journal of neurochemistry* **75**(6): 2434-2444.

Falenski KW, Blair RE, Sim-Selley LJ, Martin BR and DeLorenzo RJ (2007) Status epilepticus causes a long-lasting redistribution of hippocampal cannabinoid type 1 receptor expression and function in the rat pilocarpine model of acquired epilepsy. *Neuroscience* **146**(3): 1232-1244.

Furshpan EJ, MacLeish PR, O'Lague PH and Potter DD (1976) Chemical transmission between rat sympathetic neurons and cardiac myocytes developing in microcultures: evidence for cholinergic, adrenergic, and dual-function neurons. *Proc Natl Acad Sci U S A* **73**(11): 4225-4229.

Glass M and Northup JK (1999) Agonist selective regulation of G-proteins by cannabinoid CB1 and CB2 receptors. *Molecular pharmacology* **56**: 1362-1369.

Herkenham M, Lynn AB, Johnson MR, Melvin LS, de Costa BR and Rice KC (1991) Characterization and localization of cannabinoid receptors in rat brain: a quantitative in vitro autoradiographic study. *J Neurosci* **11**(2): 563-583.

Hirvonen J, Goodwin RS, Li CT, Terry GE, Zoghbi SS, Morse C, Pike VW, Volkow ND, Huestis MA and Innis RB (2012) Reversible and regionally selective downregulation of brain cannabinoid CB1 receptors in chronic daily cannabis smokers. *Molecular psychiatry* **17**(6): 642-649.

Howlett AC, Barth F, Bonner TI, Cabral G, Casellas P, Devane WA, Felder CC, Herkenham M, Mackie K, Martin BR, Mechoulam R and Pertwee RG (2002) International Union of Pharmacology. XXVII. Classification of cannabinoid receptors. *Pharmacol Rev* **54**(2): 161-202.

Howlett AC, Blume LC and Dalton GD (2010) CB(1) cannabinoid receptors and their associated proteins. *Curr Med Chem* **17**(14): 1382-1393.

Hsieh C, Brown S, Derleth C and Mackie K (1999) Internalization and recycling of the CB1 cannabinoid receptor. *Journal of neurochemistry* **73**(2): 493-501.

Molecular Pharmacology Fast Forward. Published on February 5, 2015 as DOI: 10.1124/mol.114.096495
This article has not been copyedited and formatted. The final version may differ from this version.

Hu SS, Arnold A, Hutchens JM, Radicke J, Cravatt BF, Wager-Miller J, Mackie K and Straiker A (2010) Architecture of cannabinoid signaling in mouse retina. *The Journal of comparative neurology* **518**(18): 3848-3866.

Jain T, Wager-Miller J, Mackie K and Straiker A (2013) Diacylglycerol lipasealpha (DAGLalpha) and DAGLbeta cooperatively regulate the production of 2-arachidonoyl glycerol in autaptic hippocampal neurons. *Molecular pharmacology* **84**(2): 296-302.

Jiang M, Deng L and Chen G (2004) High Ca(2+)-phosphate transfection efficiency enables single neuron gene analysis. *Gene Ther* **11**(17): 1303-1311.

Jin W, Brown S, Roche JP, Hsieh C, Celver JP, Kovoor A, Chavkin C and Mackie K (1999) Distinct domains of the CB1 cannabinoid receptor mediate desensitization and internalization. *J Neurosci* **19**(10): 3773-3780.

Kano M, Ohno-Shosaku T, Hashimotodani Y, Uchigashima M and Watanabe M (2009) Endocannabinoid-mediated control of synaptic transmission. *Physiol Rev* **89**(1): 309-380.

Lazenka MF, Selley DE and Sim-Selley LJ (2013) Brain regional differences in CB1 receptor adaptation and regulation of transcription. *Life Sci* **92**(8-9): 446-452.

Levison SW and McCarthy KD (1991) Characterization and partial purification of AIM: a plasma protein that induces rat cerebral type 2 astroglia from bipotential glial progenitors. *J Neurochem* **57**(3): 782-794.

Lind GE, Danielsen SA, Ahlquist T, Merok MA, Andresen K, Skotheim RI, Hektoen M, Rognum TO, Meling GI, Hoff G, Bretthauer M, Thiis-Evensen E, Nesbakken A and

Lothe RA (2011) Identification of an epigenetic biomarker panel with high sensitivity and specificity for colorectal cancer and adenomas. *Molecular cancer* **10**: 85.

Ludanyi A, Eross L, Czirjak S, Vajda J, Halasz P, Watanabe M, Palkovits M, Magloczky Z, Freund TF and Katona I (2008) Downregulation of the CB1 cannabinoid receptor and related molecular elements of the endocannabinoid system in epileptic human hippocampus. *J Neurosci* **28**(12): 2976-2990.

Martini L, Thompson D, Kharazia V and Whistler JL (2010) Differential regulation of behavioral tolerance to WIN55,212-2 by GASP1. *Neuropsychopharmacology* **35**(6): 1363-1373.

Martini L, Waldhoer M, Pusch M, Kharazia V, Fong J, Lee JH, Freissmuth C and Whistler JL (2007) Ligand-induced down-regulation of the cannabinoid 1 receptor is mediated by the G-protein-coupled receptor-associated sorting protein GASP1. *Faseb J* **21**(3): 802-811.

McDonald NA, Henstridge CM, Connolly CN and Irving AJ (2007) An essential role for constitutive endocytosis, but not activity, in the axonal targeting of the CB1 cannabinoid receptor. *Molecular pharmacology* **71**(4): 976-984.

McIntosh HH, Song C and Howlett AC (1998) CB1 canabinoid receptor: cellular regulation and distribution in N18TG2 neuroblastoma cells. *Brain Research Molecular Brain Research* **53**: 163-173.

Meschler JP, Kraichely DM, Wilken GH and Howlett AC (2000) Inverse agonist properties of N-(piperidin-1-yl)-5-(4-chlorophenyl)-1-(2, 4-dichlorophenyl)-4-methyl-1H-pyrazole-3-carboxamide HCl (SR141716A) and 1-(2-chlorophenyl)-4-cyano-5-(4-

Molecular Pharmacology Fast Forward. Published on February 5, 2015 as DOI: 10.1124/mol.114.096495
This article has not been copyedited and formatted. The final version may differ from this version.

methoxyphenyl)-1H-pyrazole-3-carboxyl ic acid phenylamide (CP-272871) for the CB(1) cannabinoid receptor [In Process Citation]. *Biochemical Pharmacology* **60**(9): 1315-1323.

Meyer AH, Katona I, Blatow M, Rozov A and Monyer H (2002) In vivo labeling of parvalbumin-positive interneurons and analysis of electrical coupling in identified neurons. *J Neurosci* **22**(16): 7055-7064.

Morgan DJ, Davis BJ, Kearn CS, Marcus D, Cook AJ, Wager-Miller J, Straiker A, Myoga MH, Karduck J, Leishman E, Sim-Selley LJ, Czyzyk TA, Bradshaw HB, Selley DE and Mackie K (2014) Mutation of putative GRK phosphorylation sites in the cannabinoid receptor 1 (CB1R) confers resistance to cannabinoid tolerance and hypersensitivity to cannabinoids in mice. *J Neurosci* **34**(15): 5152-5163.

Mukhopadhyay S and Howlett AC (2001) CB1 receptor-G protein association. Subtype selectivity is determined by distinct intracellular domains. *Eur J Biochem* **268**(3): 499-505.

Nguyen PT, Schmid CL, Raehal KM, Selley DE, Bohn LM and Sim-Selley LJ (2012) beta-arrestin2 regulates cannabinoid CB1 receptor signaling and adaptation in a central nervous system region-dependent manner. *Biological psychiatry* **71**(8): 714-724.

Nie J and Lewis DL (2001a) The proximal and distal C-terminal tail domains of the CB1 cannabinoid receptor mediate G protein coupling. *Neuroscience* **107**(1): 161-167.

Nie J and Lewis DL (2001b) Structural domains of the CB1 cannabinoid receptor that contribute to constitutive activity and G-protein sequestration. *J Neurosci* **21**(22): 8758-8764.

Niehaus JL, Liu Y, Wallis KT, Egertova M, Bhartur SG, Mukhopadhyay S, Shi S, He H, Selley DE, Howlett AC, Elphick MR and Lewis DL (2007) CB1 cannabinoid receptor activity is modulated by the cannabinoid receptor interacting protein CRIP 1a. *Molecular pharmacology* **72**(6): 1557-1566.

Oster B, Thorsen K, Lamy P, Wojdacz TK, Hansen LL, Birkenkamp-Demtroder K, Sorensen KD, Laurberg S, Orntoft TF and Andersen CL (2011) Identification and validation of highly frequent CpG island hypermethylation in colorectal adenomas and carcinomas. *International journal of cancer Journal international du cancer* **129**(12): 2855-2866.

Pacher P, Batkai S and Kunos G (2006) The endocannabinoid system as an emerging target of pharmacotherapy. *Pharmacol Rev* **58**(3): 389-462.

Rozenfeld R and Devi LA (2008) Regulation of CB1 cannabinoid receptor trafficking by the adaptor protein AP-3. *Faseb J* **22**(7): 2311-2322.

Seifert R and Wenzel-Seifert K (2002) Constitutive activity of G-protein-coupled receptors: cause of disease and common property of wild-type receptors. *Naunyn-Schmiedeberg's archives of pharmacology* **366**(5): 381-416.

Shapira M, Gafni M and Sarne Y (2003) Long-term interactions between opioid and cannabinoid agonists at the cellular level: cross-desensitization and downregulation. *Brain Res* **960**(1-2): 190-200.

Sim-Selley LJ (2003) Regulation of cannabinoid CB1 receptors in the central nervous system by chronic cannabinoids. *Critical Reviews in Neurobiology* **15**: 91-119.

Sim-Selley LJ, Brunk LK and Selley DE (2001) Inhibitory effects of SR141716A on G-protein activation in rat brain. *European journal of pharmacology* **414**(2-3): 135-143.

Sim-Selley LJ, Schechter NS, Rorrer WK, Dalton GD, Hernandez J, Martin BR and Selley DE (2006) Prolonged recovery rate of CB1 receptor adaptation after cessation of long-term cannabinoid administration. *Molecular pharmacology* **70**(3): 986-996.

Singh SN, Bakshi K, Mercier RW, Makriyannis A and Pavlopoulos S (2011) Binding between a distal C-terminus fragment of cannabinoid receptor 1 and arrestin-2. *Biochemistry* **50**(12): 2223-2234.

Smith TH, Sim-Selley LJ and Selley DE (2010) Cannabinoid CB1 receptor-interacting proteins: novel targets for central nervous system drug discovery? *Br J Pharmacol* **160**(3): 454-466.

Stauffer B, Wallis KT, Wilson SP, Egertova M, Elphick MR, Lewis DL and Hardy LR (2011) CRIP1a switches cannabinoid receptor agonist/antagonist-mediated protection from glutamate excitotoxicity. *Neuroscience letters* **503**(3): 224-228.

Straiker A, Hu SS, Long JZ, Arnold A, Wager-Miller J, Cravatt BF and Mackie K (2009) Monoacylglycerol lipase limits the duration of endocannabinoid-mediated depolarization-induced suppression of excitation in autaptic hippocampal neurons. *Molecular pharmacology* **76**(6): 1220-1227.

Molecular Pharmacology Fast Forward. Published on February 5, 2015 as DOI: 10.1124/mol.114.096495
This article has not been copyedited and formatted. The final version may differ from this version.

Straiker A and Mackie K (2005) Depolarization-induced suppression of excitation in murine autaptic hippocampal neurones. *The Journal of physiology* **569**(Pt 2): 501-517.

Straiker A and Mackie K (2009) Cannabinoid signaling in inhibitory autaptic hippocampal neurons. *Neuroscience* **163**(1): 190-201.

Straiker A, Wager-Miller J, Hutchens J and Mackie K (2012) Differential signalling in human cannabinoid CB1 receptors and their splice variants in autaptic hippocampal neurones. *Br J Pharmacol* **165**(8): 2660-2671.

Straiker AJ, Borden CR and Sullivan JM (2002) G-protein alpha subunit isoforms couple differentially to receptors that mediate presynaptic inhibition at rat hippocampal synapses. *J Neurosci* **22**(7): 2460-2468.

Sunyer T, Monastirsky B, Codina J and Birnbaumer L (1989) Studies on nucleotide and receptor regulation of Gi proteins: effects of pertussis toxin. *Mol Endocrinol* **3**(7): 1115-1124.

Tamamaki N, Yanagawa Y, Tomioka R, Miyazaki J, Obata K and Kaneko T (2003) Green fluorescent protein expression and colocalization with calretinin, parvalbumin, and somatostatin in the GAD67-GFP knock-in mouse. *The Journal of comparative neurology* **467**(1): 60-79.

Tzavara ET, Valjent E, Firmo C, Mas M, Beslot F, Defer N, Roques BP, Hanoune J and Maldonado R (2000) Cannabinoid withdrawal is dependent upon PKA activation in the cerebellum. *Eur J Neurosci* **12**(3): 1038-1046.

Molecular Pharmacology Fast Forward. Published on February 5, 2015 as DOI: 10.1124/mol.114.096495
This article has not been copyedited and formatted. The final version may differ from this version.

Villares J (2007) Chronic use of marijuana decreases cannabinoid receptor binding and mRNA expression in the human brain. *Neuroscience* **145**(1): 323-334.

Molecular Pharmacology Fast Forward. Published on February 5, 2015 as DOI: 10.1124/mol.114.096495
This article has not been copyedited and formatted. The final version may differ from this version.

Footnotes:

This work was supported by the National Institute on Drug Abuse [R21-DA025321, R01-DA003690, R03-DA035424, F31-DA023747, F31-DA032215, R01-DA011322, K05-DA021696 and T32-DA007027], the National Institute on Neurological Disorders and Stroke [T32-NS007288], the National Eye Institute [R21-EY021831], the Biotechnology and Biological Sciences Research Council [S19916], and the National Center for Advancing Translational Sciences [UL1-TR000058] in support of the A.D. Williams Fund of Virginia Commonwealth University. Mass spectrometry was supported in part with funding from the National Institute on Drug Abuse [P30-DA033934]. Rat microscopy was performed at the VCU Department of Anatomy and Neurobiology Microscopy Facility, supported in part with funding the National Institute on Neurological Disorders and Stroke [P30-NS047463].

Molecular Pharmacology Fast Forward. Published on February 5, 2015 as DOI: 10.1124/mol.114.096495
This article has not been copyedited and formatted. The final version may differ from this version.

Figure Legends

Figure 1. Quantitative $CRIP_{1a}$ immunoblots and immunohistochemical localization of $CRIP_{1a}$ in rat cerebellum. $CRIP_{1a}$ was immunologically identified by A, B) immunoblotting or C) immunofluorescence staining. Quantitative immunoblotting was conducted by comparison of a standard curve of purified $CRIP_{1a}$ with $CRIP_{1a}$ immunoreactivity in membrane homogenates from A) CB_1-HEK cells with and without stable co-transfection of $CRIP_{1a}$ or B) rat cerebellum. C) Immunofluorescence staining of $CRIP_{1a}$ (green), CB_1 receptor (red) or overlay (yellow) indicates areas of co-localization in rat cerebellum as determined by confocal microscopy. Note the characteristic scarcity of CB_1 R-ir in the granule cell layer (GCL) and co-localization of CB_1R and $CRIP_{1a}$-ir in the molecular layer (ML). Arrows indicate CB_1R-ir in perisomatic basket cell axon terminals, which are devoid of $CRIP_{1a}$-ir. GCL, granule cell layer; ML, molecular layer; PCL, Purkinje cell layer. Scale bar: 200 µm.

Figure 2. Immunohistochemical localization of $CRIP_{1a}$ in the cerebellum of GAD67-GFP transgenic mice.

A. Overview of $CRIP_{1a}$ staining versus GAD67-GFP in murine cerebellum shows a broad distribution in both the molecular and granular layers. B. $CRIP_{1a}$ distribution near Purkinje cells. C. $CRIP_{1a}$ protein in granular layer. D. $CRIP_{1a}$ overlaps substantially with presynaptic marker SV2 in the molecular layer. E. In the adjacent image, $CRIP_{1a}$ also partially overlaps with GAD67-GFP neurons (arrows), including likely Purkinje cell processes. F. Sample of CB_1R colocalization with $CRIP_{1a}$ (arrows) in the molecular

Molecular Pharmacology Fast Forward. Published on February 5, 2015 as DOI: 10.1124/mol.114.096495
This article has not been copyedited and formatted. The final version may differ from this version.

layer near Purkinje cells. Purkinje pinceau region is dense with CB_1 (arrowhead). Scale bars: A: 100 µm; B: 25 µm; C: 30 µm; and D-F: 10 µm.

Figure 3. Co-localization of $CRIP_{1a}$ with CB_1R, SV2, GAD65 and Parvalbumin in the murine cerebellar granule cell layer. A. Staining of $CRIP_{1a}$ (green) versus CB_1R (red) shows numerous points of overlap in the granular layer of the murine cerebellum (arrows). But there are also clear cases where CB_1R expression does not overlap with $CRIP_{1a}$ (arrowheads). Even punctate $CRIP_{1a}$ staining that appears to be green is often accompanied by CB_1R staining (e.g. left arrow). Note larger CB_1R-positive structures correspond to pinceau staining. B. $CRIP_{1a}$ (green) is commonly associated with the presynaptic marker SV2 (red), both in the bright staining corresponding to mossy terminals but also, if the image is allowed to saturate as in this case, with a subset of isolated puncta (arrows). However non-overlap also occurs (arrowheads). C) $CRIP_{1a}$ (green) does not overlap with GAD65 (red) staining (arrows). D) $CRIP_{1a}$ is absent in the pinceau region as identified by GAD65 staining (D1). Purkinje cell is marked by an asterisk. Scale bars: A1: 35 µm; A2-4: 15 µm ; B1: 25 µm; B2-4: 10 µm; C: 20 µm; D: 5 µm.

Figure 4. Effects of $CRIP_{1a}$ over-expression on concentration-effect curves of ligand-modulated [^{35}S]GTPγS binding in CB_1-HEK cell membranes. Membranes from CB_1-HEK cells with (open symbols) and without (closed symbols) stable co-transfection of $CRIP_{1a}$ were incubated (as described in Methods) with 100 mM NaCl, 10 µM GDP, 0.1 nM [^{35}S]GTPγS and varying concentrations of the indicated ligands: A) noladin ether (2-

Molecular Pharmacology Fast Forward. Published on February 5, 2015 as DOI: 10.1124/mol.114.096495
This article has not been copyedited and formatted. The final version may differ from this version.

AGE) and CP55,940 (CP); B) WIN55,212-2 (WIN) or methanandamide (MAEA); or C) Δ^9-tetrahydrocannabinol (THC) or rimonabant (RIM). Data are mean % stimulation ± SEM (n = 3-6). No CRIP, no transfection of $CRIP_{1a}$; $CRIP_{1a}$, stable transfection of $CRIP_{1a}$.

Figure 5. $CRIP_{1a}$ over-expression in CB_1-HEK cells suppressed basal [^{35}S]GTPγS binding in the absence of sodium in a PTX-sensitive manner. Membranes from CB_1-HEK cells with and without stable co-transfection of $CRIP_{1a}$ were pretreated for 24 hr with and without 50 ng/ml PTX, then were incubated with 10 µM GDP, 0.1 nM [^{35}S]GTPγS in the presence and absence of 100 mM NaCl (as described in Methods). Data are mean fmol/mg bound ± SEM (n = 4). *, $p < 0.05$ different from cells without $CRIP_{1a}$ co-transfection under the corresponding conditions, as determined by two-way ANOVA with Bonferroni post-hoc test. No CRIP, no transfection of $CRIP_{1a}$; $CRIP_{1a}$, stable transfection of $CRIP_{1a}$.

Figure 6. $CRIP_{1a}$ over-expression in CB_1-HEK cells affects net ligand-modulated [^{35}S]GTPγS binding in a sodium-dependent manner. Membranes from CB_1-HEK cells with and without stable co-transfection of $CRIP_{1a}$ were incubated with 10 µM GDP, 0.1 nM [^{35}S]GTPγS in the presence and absence of 100 mM NaCl (as described in Methods). Data are mean fmol/mg bound ± SEM (n = 4-5). *, $p < 0.05$ different from cells without $CRIP_{1a}$ co-transfection under the corresponding conditions, as determined by two-way ANOVA with Bonferroni post-hoc test. No CRIP, no transfection of $CRIP_{1a}$; $CRIP_{1a}$, stable transfection of $CRIP_{1a}$.

Molecular Pharmacology Fast Forward. Published on February 5, 2015 as DOI: 10.1124/mol.114.096495
This article has not been copyedited and formatted. The final version may differ from this version.

Figure 7. $CRIP_{1a}$ does not affect ligand-induced desensitization of CB_1R-mediated G-protein activation in CB_1-HEK cells. Cells were pretreated for 4 hr with 10 µM WIN55,212-2, 6 µM THC or vehicle prior to harvesting and preparation of membranes. Varying concentrations of MAEA were incubated with membranes prepared from the indicated cell lines in the presence of 100 mM NaCl, 10 µM GDP and 0.1 nM [^{35}S]GTPγS, as described in Methods. Data are mean % stimulation ± SEM (n = 4). No CRIP, no transfection of $CRIP_{1a}$; $CRIP_{1a}$, stable transfection of $CRIP_{1a}$.

Figure 8. Effect of $CRIP_{1a}$ knockdown and over-expression on concentration-effect curves of ligand-modulated [^{35}S]GTPγS binding in N18TG2 neuroblastoma cell membranes. Membranes from wild-type N18TG2 cells or N18TG2 cells with siRNA-mediated knockdown ($CRIP_{1a}$-KD; clone 2C) or overexpression ($CRIP_{1a}$-OX; clone 1) of $CRIP_{1a}$ were incubated as described in Methods with 100 mM NaCl, 20 µM GDP, 0.1 nM [^{35}S]GTPγS and varying concentrations of WIN55,212-2 (WIN), methanandamide (MAEA) or rimonabant (RIM). Data are mean % stimulation ± SEM (n = 5-9).

Figure 9. $CRIP_{1a}$ partially co-localizes with CB_1R in autaptic hippocampal neurons. A. Micrograph in transfected autaptic hippocampal neuron shows HA11 staining of transfected HA-$CRIP_{1a}$ (green) in a mCherry-labeled (red) neuron, indicating that $CRIP_{1a}$ is expressed throughout the transfected neuron. Right panel: Nomarski image of the island is shown for reference. Scale bar: 20 µm. B. Endogenous $CRIP_{1a}$ (green) and CB_1R (red) staining in an untransfected autaptic hippocampal neuron (overlap in

Molecular Pharmacology Fast Forward. Published on February 5, 2015 as DOI: 10.1124/mol.114.096495
This article has not been copyedited and formatted. The final version may differ from this version.

yellow). C. DIC image corresponding to B. Scale bar: 15 µm. D-E. $CRIP_{1a}$ (left panel) and CB_1R (right panel) staining from B. Arrows indicate overlap. F. Zoom from inset box in B. Scale bar: 3 µm.

Figure 10. Over expression of $CRIP_{1a}$ diminishes CB_1-mediated DSE in autaptic hippocampal neurons. A) DSE time-courses for WT (red) vs. $CRIP_{1a}$ transfected neurons (black) in response to 3 sec depolarization (arrow). Insets show sample EPSCs from control (1), maximal DSE inhibition (2) and recovery (3) for $CRIP_{1a}$ transfected (left) and WT (right) neurons. B) "Dose" response for DSE using a range of depolarizations from 50 ms to 10 sec. The wild type DSE dose response is shown for comparison. *, $p < 0.05$ Bonferroni post-hoc test, 2-way ANOVA. C) Bar graph shows relative EPSC charge (1.0 = baseline, no inhibition) after treatment with three drugs under WT and CRIP1a-transfected conditions: cyclopentyladenosine (CPA, 100nM); 2-AG (5µM); MetAEA (5µM). *, $p<0.05$, unpaired t-test.

Molecular Pharmacology Fast Forward. Published on February 5, 2015 as DOI: 10.1124/mol.114.096495
This article has not been copyedited and formatted. The final version may differ from this version.

Table 1. Stoichiometry of $CRIP_{1a}$ and CB_1 receptor expression in CB_1-HEK and CB_1-HEK-$CRIP_{1a}$ cells compared to rat cerebellum

Tissue Source	CB_1 B_{max} (pmol/mg)	CB_1 K_D (nM)	$CRIP_{1a}$ (pmol/mg)	Molar Ratio $CRIP_{1a}/CB_1$
CB_1-HEK	1.34 ± 0.12	1.45 ± 0.19	0.56 ± 0.13	0.42 ± 0.09
CB_1-HEK-$CRIP_{1a}$	1.17 ± 0.13	1.63 ± 0.35	8.20 ± 0.64**	7.01 ± 0.55**
Rat Cerebellum	3.76 ± 0.31	0.49 ± 0.04	115 ± 12.2	32.02 ± 4.39

Membranes prepared from the indicated tissue sources were incubated with varying concentrations of [^{3}H]SR141716A, as described in Methods. B_{max} and K_D values were derived from non-linear regression analysis of the saturation binding curves. $CRIP_{1a}$ protein values were determined by quantitative immunoblot of the indicated tissue source, using purified $CRIP_{1a}$ as an internal standard, as described in Methods. Data are mean values ± SEM (n = 4-6). **, $p < 0.01$ different from corresponding value in CB_1-HEK cells by Student's *t*-test with Welch's correction (note: values from cerebellum were not included in the analysis).

Molecular Pharmacology Fast Forward. Published on February 5, 2015 as DOI: 10.1124/mol.114.096495
This article has not been copyedited and formatted. The final version may differ from this version.

Table 2. E_{max} and EC_{50} values of ligand-modulated [^{35}S]GTPγS binding in CB_1-HEK and CB_1-HEK-$CRIP_{1a}$ cells

Cell line:	CB_1-HEK		CB_1-HEK-$CRIP_{1a}$		
Ligand	E_{max} (% Stim)	EC_{50} (nM)	E_{max} (% Stim)	EC_{50} (nM)	p value
2-AGE	137.7 ± 9.7[a]	59.9 ± 3.8	108.2 ± 3.7[a] *	104 ± 16	<0.0001
HU210	114.6 ± 5.9[ab]	0.04 ± 0.01	96.0 ± 6.1[b §]	0.06 ± 0.01	<0.0001
WIN55,212-2	112.7 ± 8.8[abc]	110 ± 41	79.5 ± 1.7[c] *	90.6 ± 6.2	<0.0001
CP55,940	100.0 ± 8.7[bc]	48.8 ± 2.2	72.0 ± 2.7[c] *	51.4 ± 6.3	<0.0001
MAEA	73.8 ± 6.1[c]	202 ± 37	73.0 ± 6.0[c]	255 ± 40	0.4928
Levonantradol	73.7 ± 11.3[c]	34.2 ± 8.6	72.8 ± 0.5[c]	19.0 ± 5.2	0.2360
THC	19.6 ± 2.7[d]	11.5 ± 2.4	20.4 ± 3.1[d]	8.1 ± 1.2	0.1740
Rimonabant	-12.9 ± 1.5	1.0 ± 0.4	-6.5 ± 1.5 *	0.5 ± 0.1	0.0002

Varying concentrations of the indicated ligands were incubated with membranes prepared from the indicated cell lines in the presence of 10 µM GDP and 0.1 nM [^{35}S]GTPγS, as described in Methods. E_{max} and EC_{50} values were derived from non-linear regression analysis of ligand concentration-effect curves. Data are mean values ± SEM (n = 3-6). The p values in the rightmost column denote significance of the effect of $CRIP_{1a}$ over-expression, derived from 2-way ANOVA (ligand concentration x cell line) of the concentration effect curves. Values <0.05 are considered significant. Significance of E_{max} and EC_{50} values between cell lines were determined by Student's *t*-test, and denoted by the following symbols. *, $p < 0.05$ different from CB_1-HEK cells. [§], $p = 0.05$ different from CB_1-HEK cells. Significant differences between ligand E_{max} values within

Molecular Pharmacology Fast Forward. Published on February 5, 2015 as DOI: 10.1124/mol.114.096495
This article has not been copyedited and formatted. The final version may differ from this version.

each cell line are denoted as follows: ligands without any similar letter designations are $p < 0.05$ different from each other as determined by 1-way ANOVA with post-hoc Newman-Keuls test.

Molecular Pharmacology Fast Forward. Published on February 5, 2015 as DOI: 10.1124/mol.114.096495
This article has not been copyedited and formatted. The final version may differ from this version.

Table 3. Curve-fit values of MAEA-stimulated [^{35}S]GTPγS and [^{3}H]SR141716A binding in CB_1-HEK and CB_1-HEK-$CRIP_{1a}$ cells pretreated with vehicle, WIN55,212-2 or THC

A. E_{max} and EC_{50} values of MAEA-stimulated [^{35}S]GTPγS binding

Cell line:	CB_1-HEK		CB_1-HEK-$CRIP_{1a}$	
Pretreatment	E_{max} (% Stim)	EC_{50} (nM)	E_{max} (% Stim)	EC_{50} (nM)
Vehicle	128.5 ± 8.0	308 ± 71	112.6 ± 5.1	423 ± 82
WIN55,212-2	42.7 ± 6.9**	5412 ± 1870§	36.9 ± 4.5**	4112 ± 633§§
THC	100.5 ± 8.5	4609 ± 2137§	104.3 ± 7.3	5175 ± 1316§§

B. B_{max} and K_D values of [^{3}H]SR141716A binding

Cell line:	CB_1-HEK		CB_1-HEK-$CRIP_{1a}$	
Pretreatment	B_{max} (pmol/mg)	K_D (nM)	B_{max} (pmol/mg)	K_D (nM)
Vehicle	1.19 ± 0.11	1.78 ± 0.23	0.97 ± 0.15	1.72 ± 0.46
WIN55,212-2	0.56 ± 0.10**	1.37 ± 0.34	0.86 ± 0.14	2.18 ± 0.69
THC	0.31 ± 0.04**	1.78 ± 0.59	0.62 ± 0.12	2.40 ± 1.07

Cells were pretreated for 4 hr with 10 µM WIN55,212-2, 6 µM THC or vehicle. A) Varying concentrations of MAEA were incubated with membranes prepared from the indicated cell lines in the presence of 10 µM GDP and 0.1 nM [^{35}S]GTPγS, as described

Molecular Pharmacology Fast Forward. Published on February 5, 2015 as DOI: 10.1124/mol.114.096495
This article has not been copyedited and formatted. The final version may differ from this version.

in Methods. B) Varying concentrations of [^{3}H]SR141716A were incubated with membranes prepared from the indicated cell lines, as described in Methods. E_{max}, EC_{50}, B_{max} and K_D values were derived from non-linear regression analysis of the concentration-effect (A) or saturation binding (B) curves. Data are mean values ± SEM (n = 4-5). *, **, ***, MAEA E_{max} or [^{3}H]SR141716A B_{max} values are $p < 0.05$, 0.01 or 0.001 different from vehicle-treated cells of the same type, as determined by 1-way ANOVA with post-hoc Dunnett's test. §,§§ , MAEA EC_{50} values are p = 0.05, 0.01 different from vehicle-treated cells of the same type, as determined by 1-way ANOVA of square root transformed data with post-hoc Dunnett's test. No significant differences in [^{3}H]SR141716A K_D values were detected by 1-way ANOVA.

Molecular Pharmacology Fast Forward. Published on February 5, 2015 as DOI: 10.1124/mol.114.096495
This article has not been copyedited and formatted. The final version may differ from this version.

Table 4. Stoichiometry of $CRIP_{1a}$ and CB_1 receptor expression in N18TG2 and N18TG2-$CRIP_{1a}$ cells

Tissue Source	CB_1 B_{max} (pmol/mg)	CB_1 K_D (nM)	$CRIP_{1a}$ (pmol/mg)	Molar Ratio $CRIP_{1a}/CB_1$
Control N18TG2	0.298 ± 0.039	2.35 ± 0.33	0.56 ± 0.07	1.87 ± 0.23
N18-$CRIP_{1a}$-OX1	0.277 ± 0.033	3.02 ± 0.71	1.35 ± 0.16**	4.87 ± 0.59**
N18-$CRIP_{1a}$-OX5	0.270 ± 0.050	4.22 ± 0.96	1.28 ± 0.09**	4.74 ± 0.34**
N18-$CRIP_{1a}$-KD	0.320 ± 0.045	2.49 ± 0.38	N.D.	N.D.

Membranes prepared from the indicated cell line were incubated with varying concentrations of [^{3}H]CP55,940, as described in Methods. B_{max} and K_D values were derived from non-linear regression analysis of the saturation binding curves. $CRIP_{1a}$ protein values were determined by quantitative immunoblot using purified $CRIP_{1a}$ as an internal standard, as described in Methods. Data are mean values ± SEM (n = 4-8). **, $p < 0.01$ different from corresponding value in control N18TG2 cells by 1-way ANOVA with post-hoc Dunnett's test. N.D., not determined.

Molecular Pharmacology Fast Forward. Published on February 5, 2015 as DOI: 10.1124/mol.114.096495
This article has not been copyedited and formatted. The final version may differ from this version.

Table 5. E_{max} and EC_{50} values of ligand-stimulated [^{35}S]GTPγS binding in N18TG2 cells with and without stable over-expression or knockdown of $CRIP_{1a}$

Ligand:	WIN55,212-2		MAEA	
Cell Line	E_{max} (% Stim)	EC_{50} (nM)	E_{max} (% Stim)	EC_{50} (nM)
WT-N18TG2	45.1 ± 5.5	53.8 ± 12.2	40.1 ± 5.3	497 ± 197
N18-$CRIP_{1a}$-OX	26.0 ± 3.5*	82.5 ± 8.9	30.2 ± 3.5	594 ± 178
N18-$CRIP_{1a}$-KD	64.0 ± 8.5*§§	40.9 ± 8.3	56.2 ± 5.3*§	322 ± 71

Varying concentrations of WIN55,212-2 or MAEA were incubated with membranes prepared from the indicated cell lines in the presence of 20 µM GDP and 0.1 nM [^{35}S]GTPγS, as described in Methods. E_{max} and EC_{50} values were derived from non-linear regression analysis of ligand concentration-effect curves. Data are mean values ± SEM (n = 5-9). Significance of E_{max} and EC_{50} values between cell-types were determined by 1-way ANOVA with post-hoc Newman-Keuls test. *, $p < 0.05$ different from WT-N18TG2 cells. §, §§, $p < 0.05$, $p < 0.01$ different from N18-$CRIP_{1a}$-OX cells. Key: WT-N18TG2, wild-type N18TG2 cells; N18-$CRIP_{1a}$-OX, N18TG2 cells over-expressing $CRIP_{1a}$ (clone 1); N18-$CRIP_{1a}$-KD, N18TG2 cells with siRNA-mediated knockdown of $CRIP_{1a}$ (clone 2C).

Figure 1

A

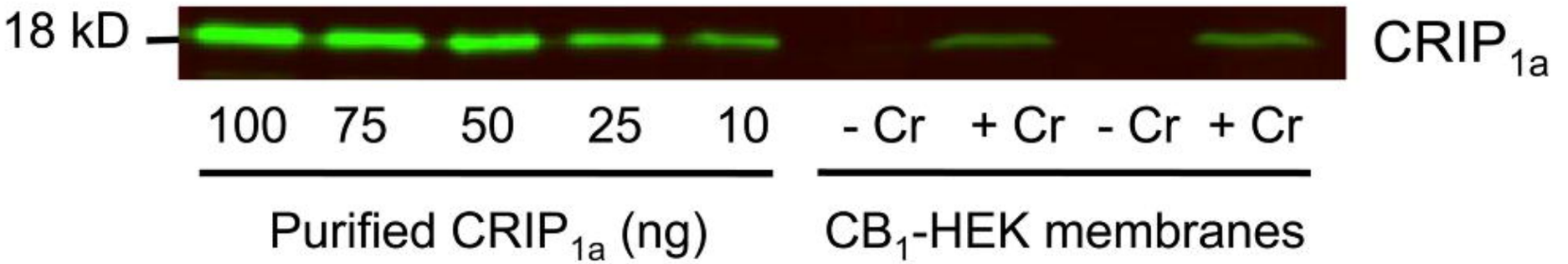
18 kD
CRIP1a
100 75 50 25 10
- Cr + Cr - Cr + Cr
Purified CRIP1a (ng)
CB1-HEK membranes

B

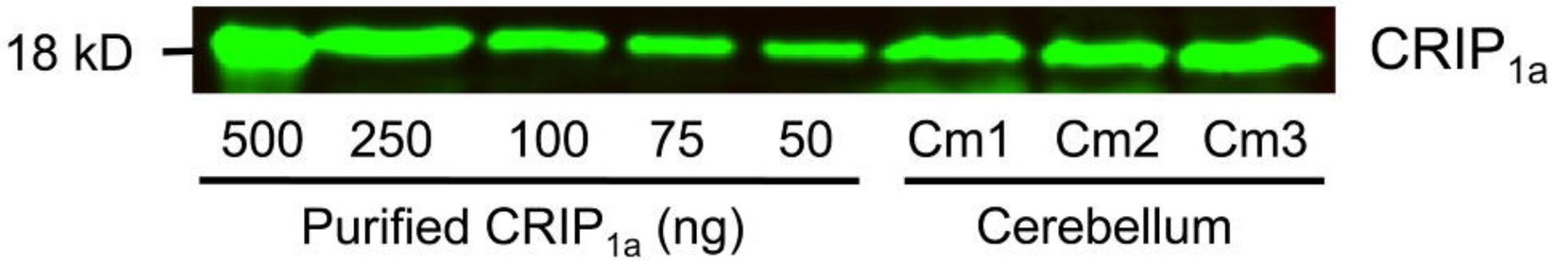
18 kD
CRIP1a
500 250 100 75 50
Cm1 Cm2 Cm3
Purified CRIP1a (ng)
Cerebellum

C

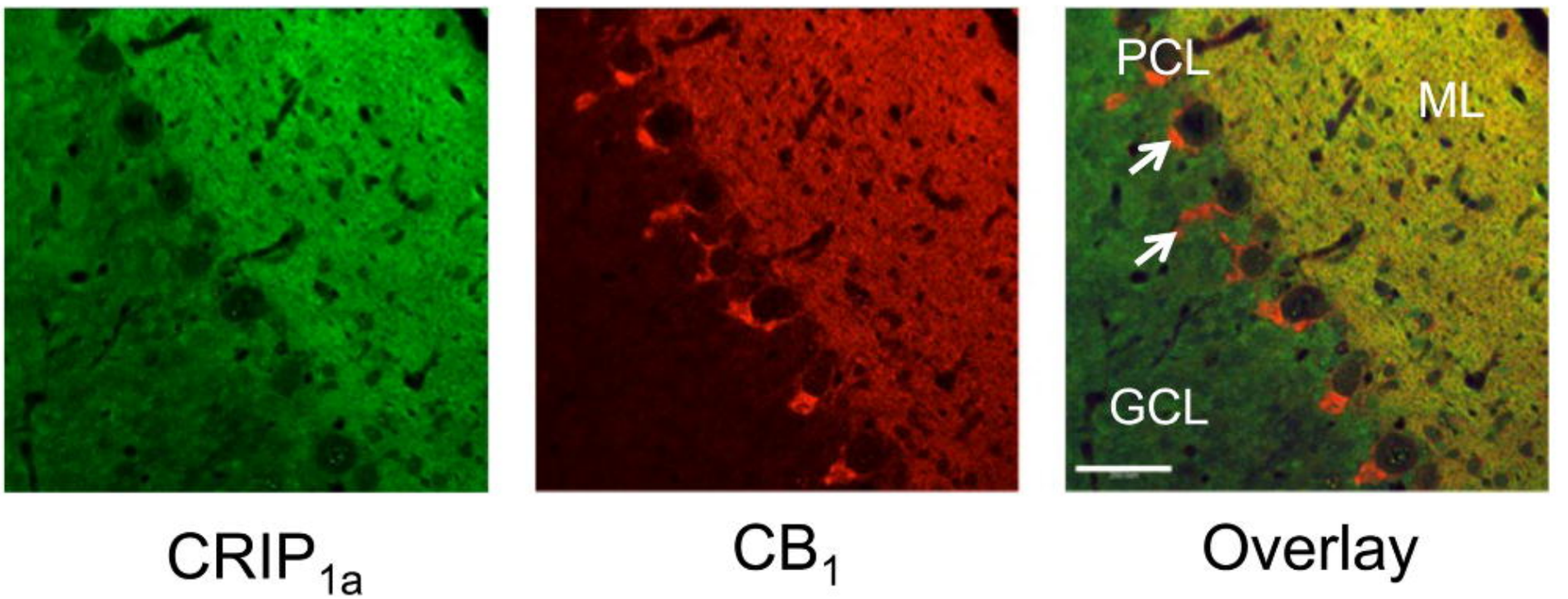
PCL
ML
GCL
CRIP1a
CB1
Overlay

Figure 2

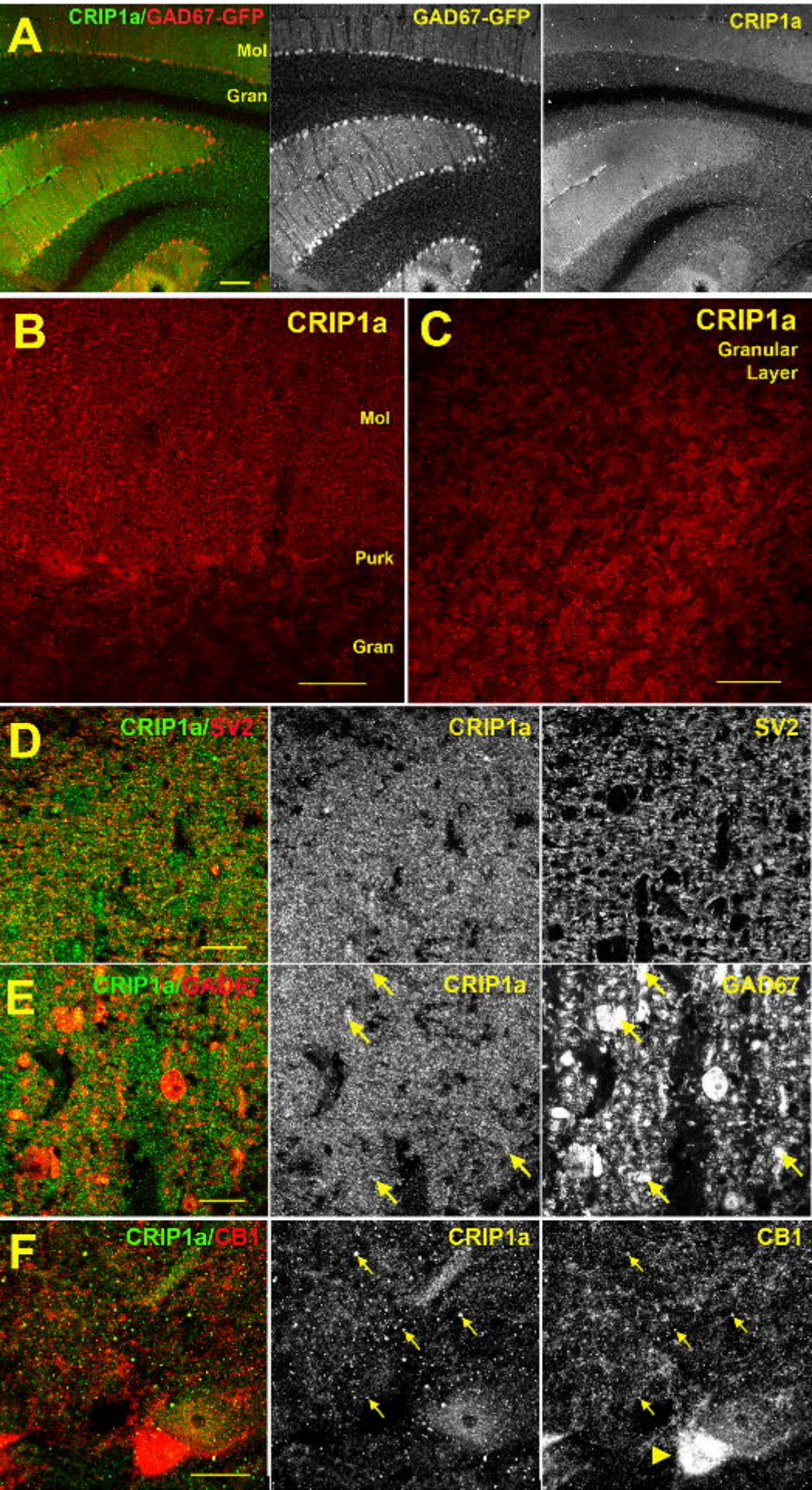
A
CRIP1a/GAD67-GFP
Mol
Gran
GAD67-GFP
CRIP1a
B
CRIP1a
Mol
Purk
Gran
C
CRIP1a
Granular
Layer
D
CRIP1a/SV2
CRIP1a
SV2
E
CRIP1a/GAD67
CRIP1a
GAD67
F
CRIP1a/CB1
CRIP1a
CB1

Figure 3

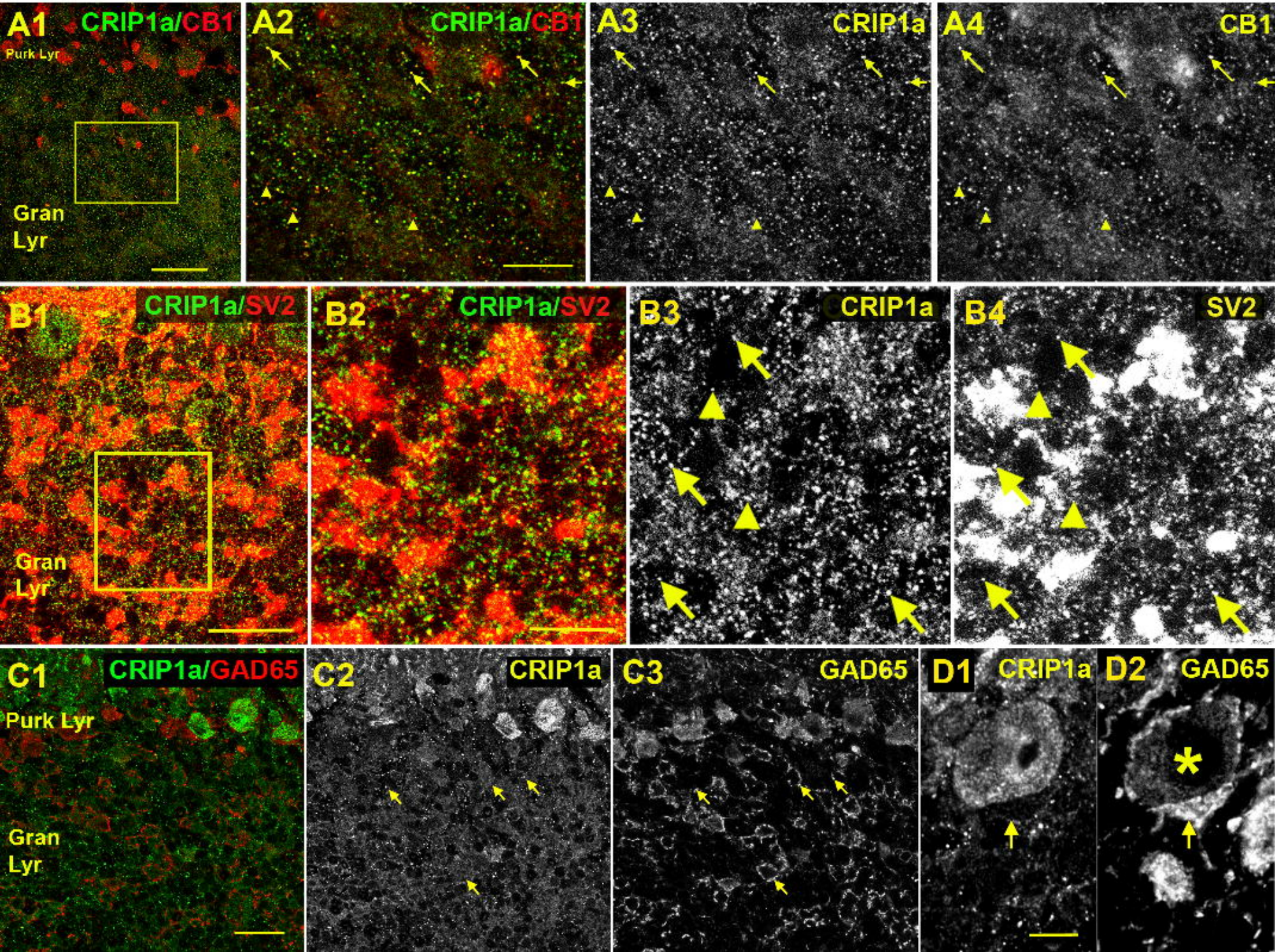
A1
CRIP1a/CB1
Purk Lyr
Gran Lyr
A2
CRIP1a/CB1
A3
CRIP1a
A4
CB1
B1
CRIP1a/SV2
Gran Lyr
B2
CRIP1a/SV2
B3
CRIP1a
B4
SV2
C1
CRIP1a/GAD65
Purk Lyr
Gran Lyr
C2
CRIP1a
C3
GAD65
D1
CRIP1a
D2
GAD65
*

Figure 4

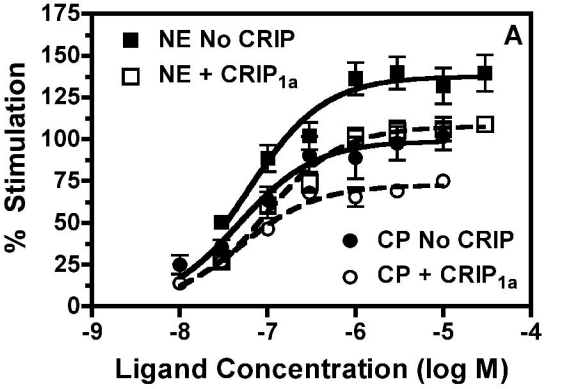
A
NE No CRIP
NE + CRIP1a
CP No CRIP
CP + CRIP1a
% Stimulation
Ligand Concentration (log M)
175
150
125
100
75
50
25
0
-9
-8
-7
-6
-5
-4

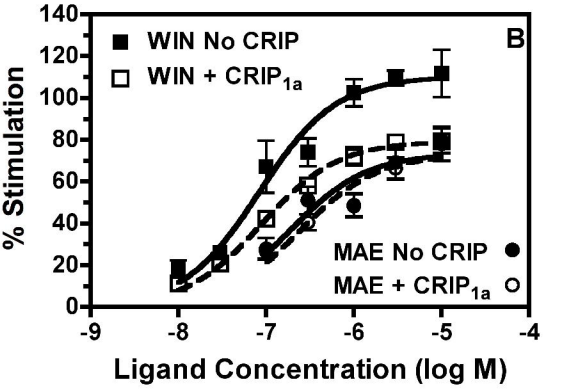
B
WIN No CRIP
WIN + CRIP1a
MAE No CRIP
MAE + CRIP1a
% Stimulation
Ligand Concentration (log M)
140
120
100
80
60
40
20
0
-9
-8
-7
-6
-5
-4

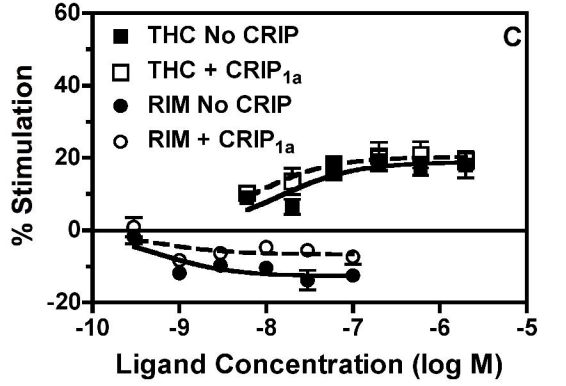
C
THC No CRIP
THC + CRIP1a
RIM No CRIP
RIM + CRIP1a
% Stimulation
Ligand Concentration (log M)
60
40
20
0
-20
-10
-9
-8
-7
-6
-5

Figure 5

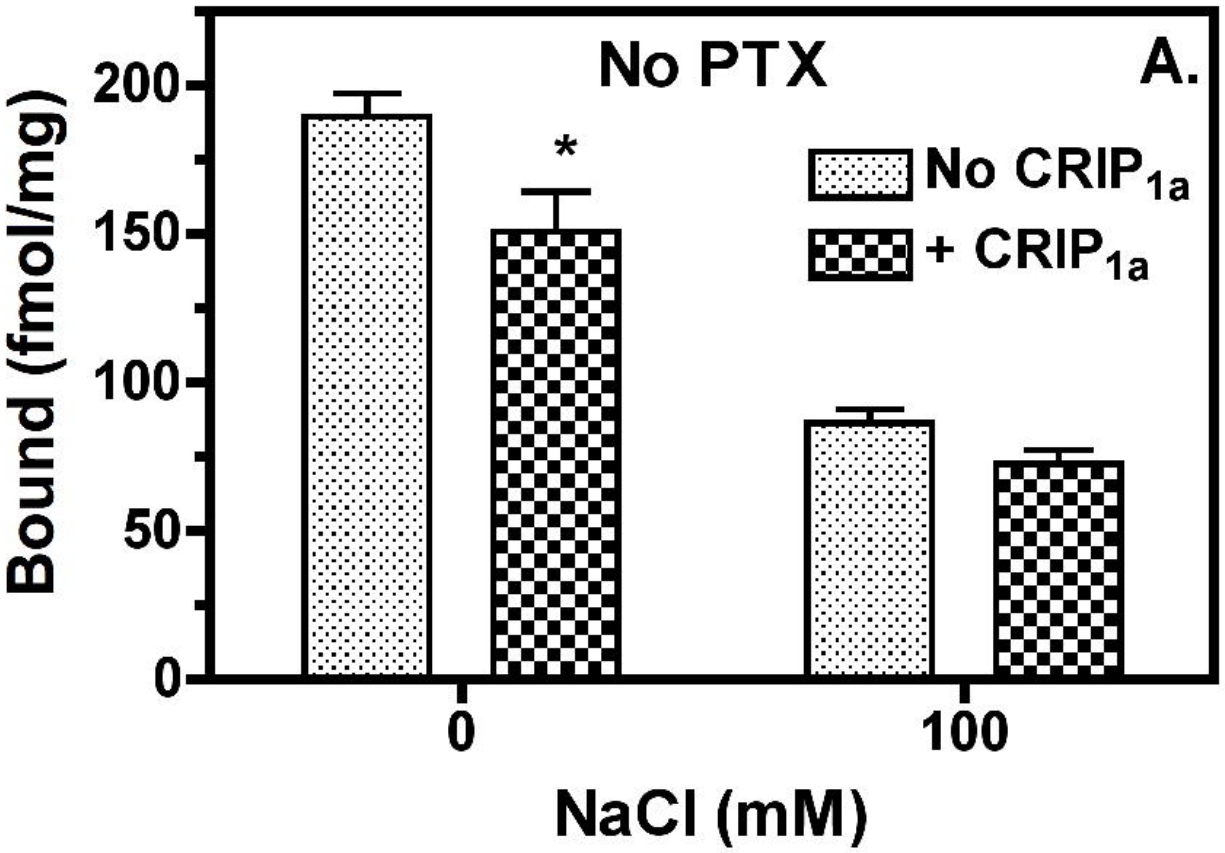
No PTX
A.
*
No CRIP1a
+ CRIP1a
Bound (fmol/mg)
200
150
100
50
0
0
100
NaCl (mM)

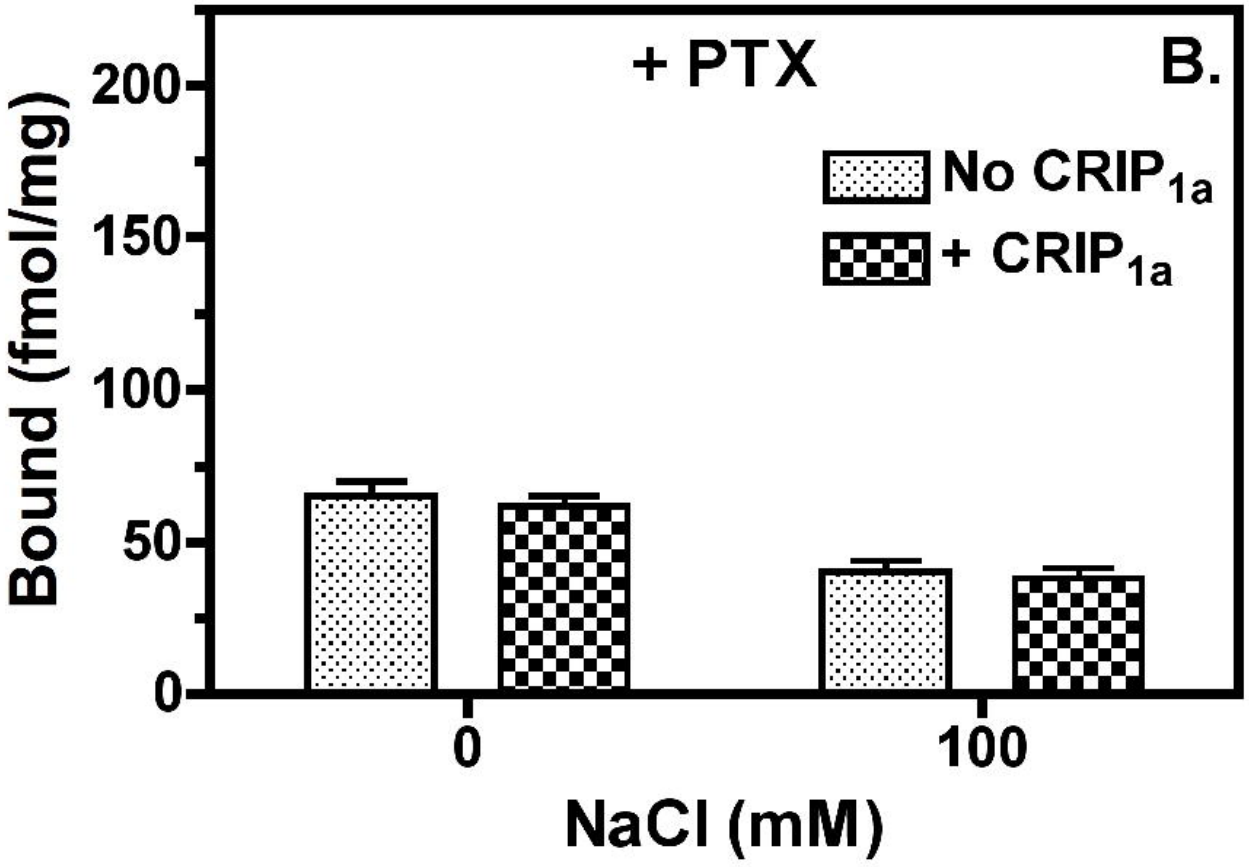
+ PTX
B.
No CRIP1a
+ CRIP1a
Bound (fmol/mg)
200
150
100
50
0
0
100
NaCl (mM)

Figure 6

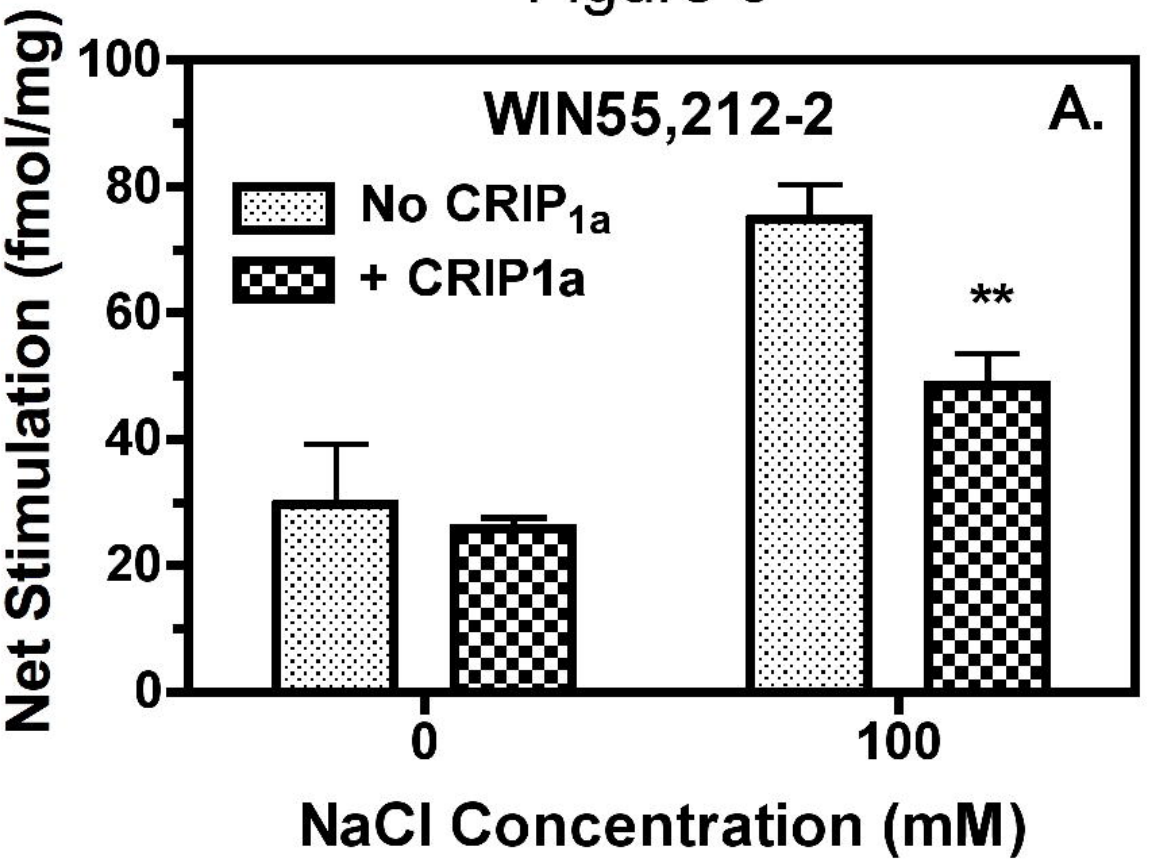
WIN55,212-2
A.
No CRIP1a
+ CRIP1a
**
Net Stimulation (fmol/mg)
100
80
60
40
20
0
0
100
NaCl Concentration (mM)

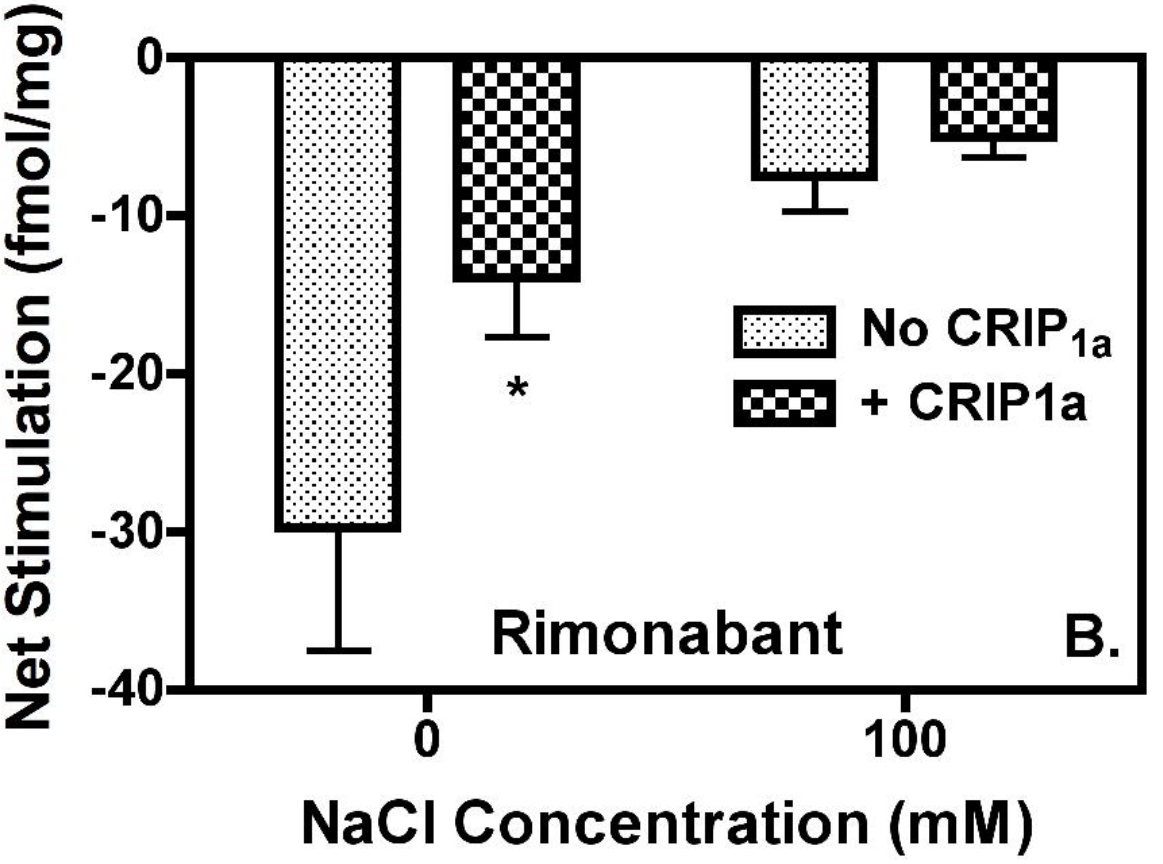
No CRIP1a
+ CRIP1a
*
Rimonabant
B.
Net Stimulation (fmol/mg)
0
-10
-20
-30
-40
0
100
NaCl Concentration (mM)

Figure 7

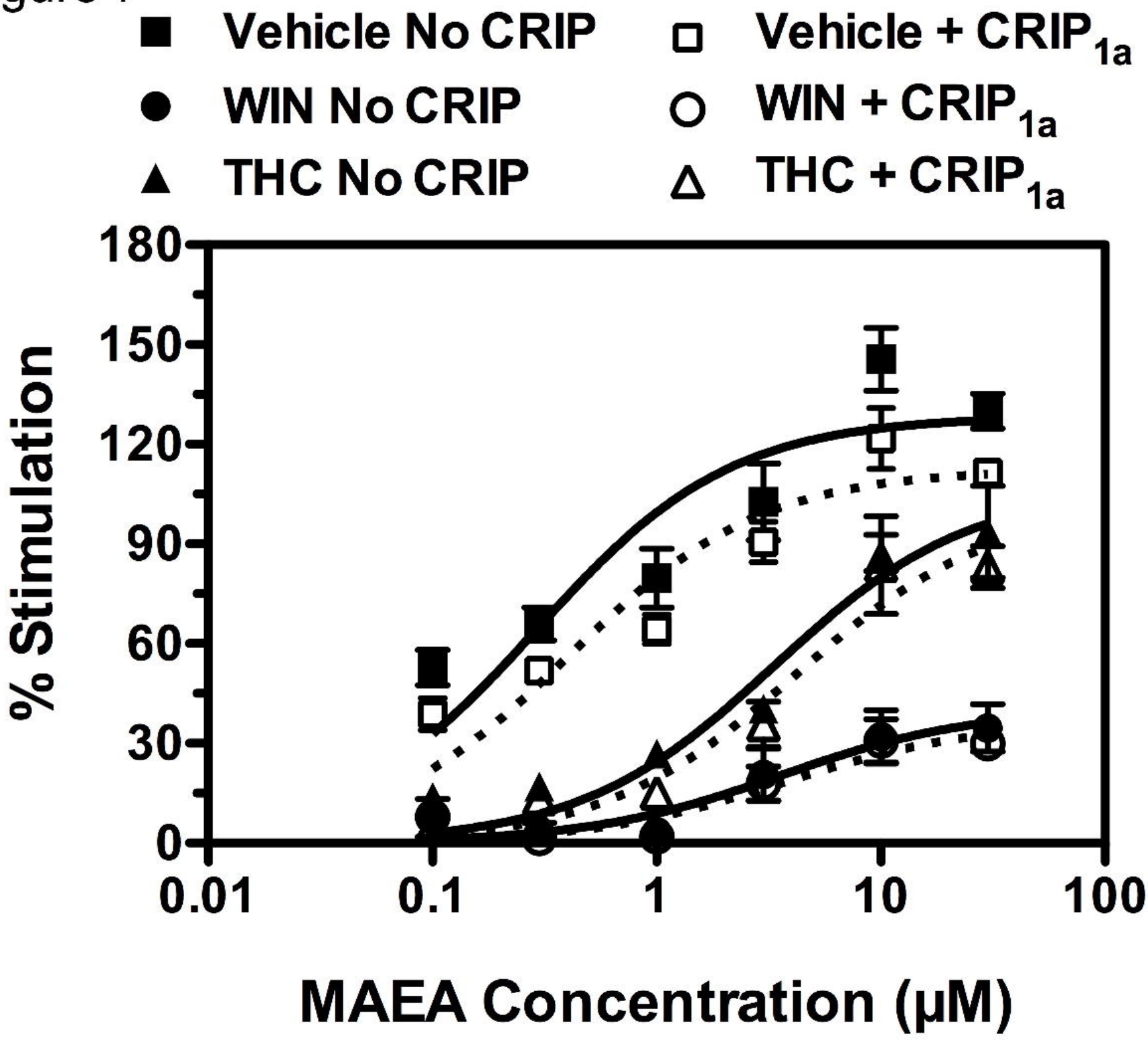
Vehicle No CRIP
Vehicle + CRIP1a
WIN No CRIP
WIN + CRIP1a
THC No CRIP
THC + CRIP1a
% Stimulation
180
150
120
90
60
30
0
0.01
0.1
1
10
100
MAEA Concentration (μM)

Figure 8

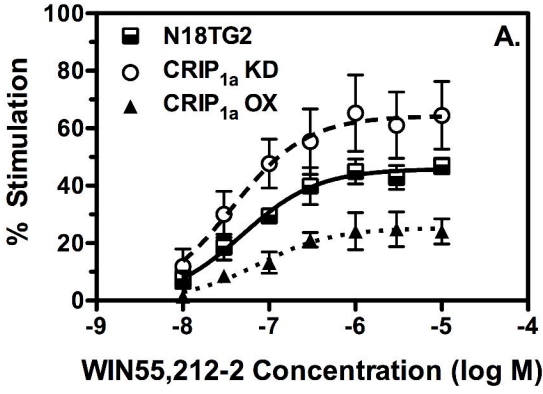
A.
N18TG2
CRIP1a KD
CRIP1a OX
% Stimulation
100
80
60
40
20
0
-9
-8
-7
-6
-5
-4
WIN55,212-2 Concentration (log M)

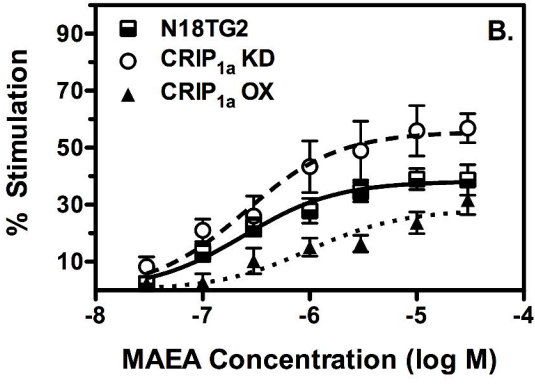
B.
N18TG2
CRIP1a KD
CRIP1a OX
% Stimulation
90
70
50
30
10
-8
-7
-6
-5
-4
MAEA Concentration (log M)

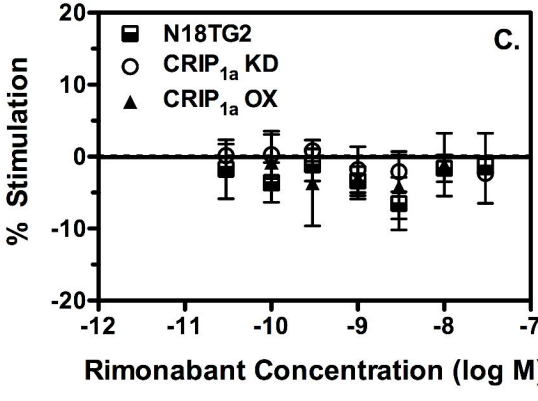
C.
N18TG2
CRIP1a KD
CRIP1a OX
% Stimulation
20
10
0
-10
-20
-12
-11
-10
-9
-8
-7
Rimonabant Concentration (log M)

Figure 9

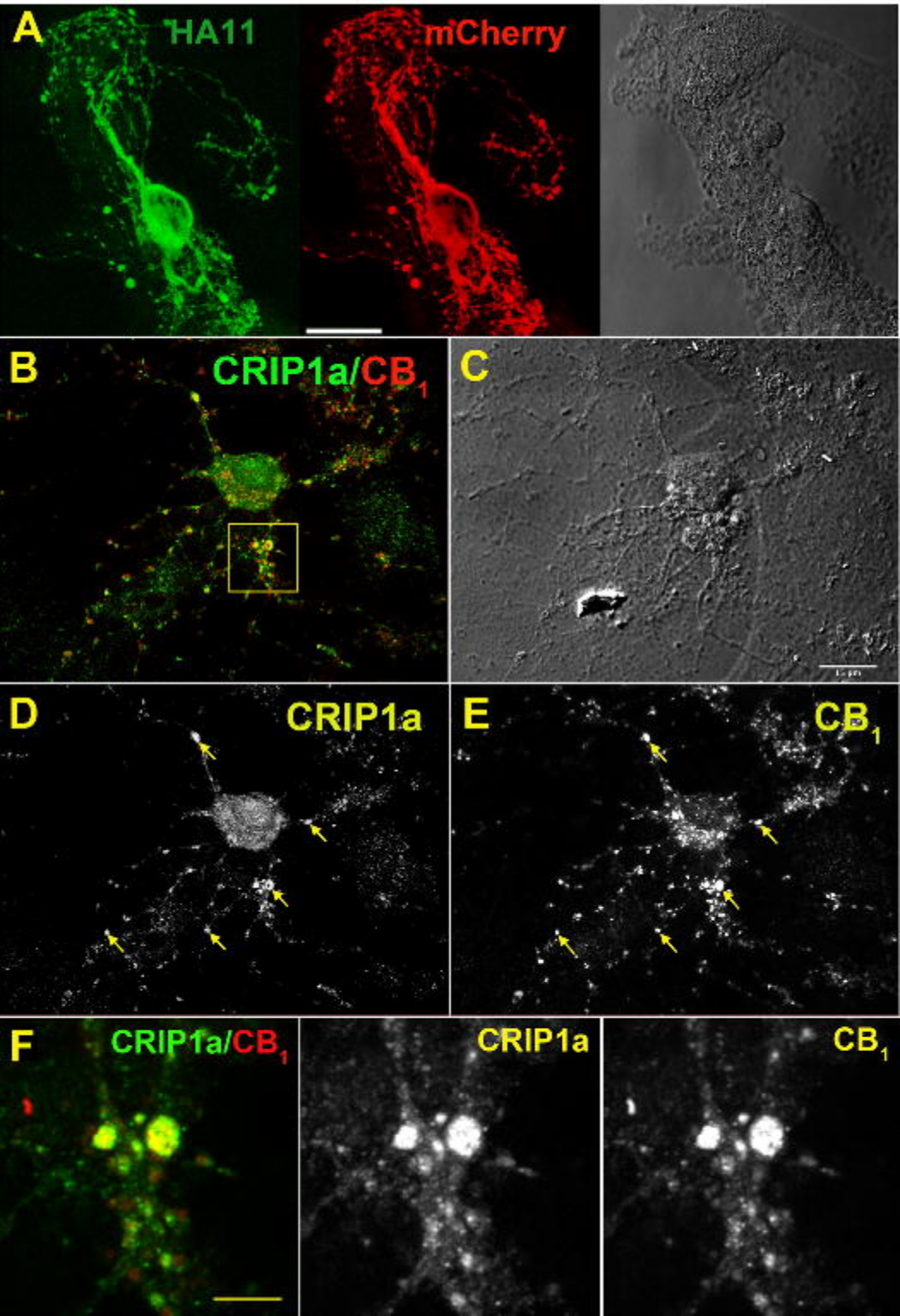
A
HA11
mCherry
B
CRIP1a/CB1
C
D
CRIP1a
E
CB1
F
CRIP1a/CB1
CRIP1a
CB1

Figure 10

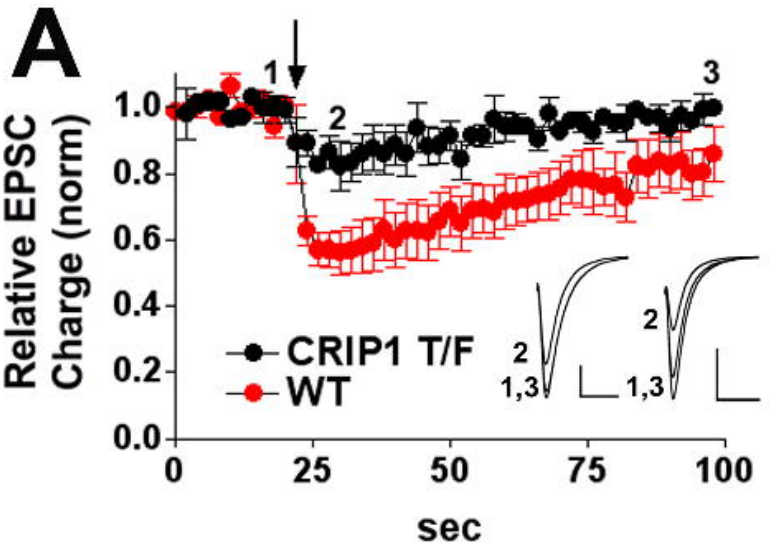
A
Relative EPSC Charge (norm)
1.0
0.8
0.6
0.4
0.2
0.0
0
25
50
75
100
sec
1
2
3
CRIP1 T/F
WT
2
1,3
2
1,3

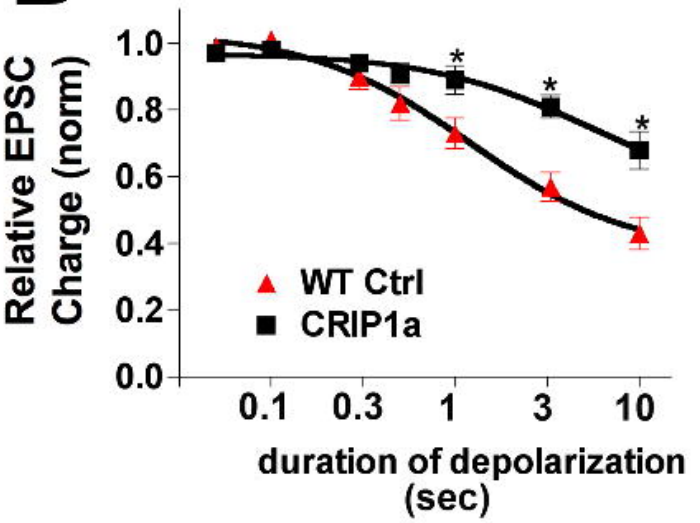
B
Relative EPSC Charge (norm)
1.0
0.8
0.6
0.4
0.2
0.0
0.1
0.3
1
3
10
duration of depolarization (sec)
WT Ctrl
CRIP1a
*
*
*

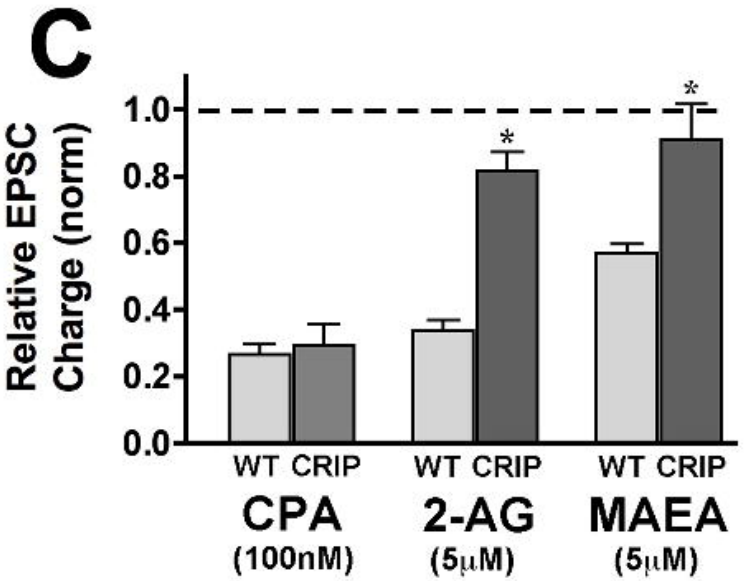
C
Relative EPSC Charge (norm)
1.0
0.8
0.6
0.4
0.2
0.0
*
*
WT CRIP
WT CRIP
WT CRIP
CPA
(100nM)
2-AG
(5μM)
MAEA
(5μM)